

Joint Active and Passive Beamforming Design for IRS-Aided Radar-Communication

Meng Hua[✉], Qingqing Wu[✉], *Senior Member, IEEE*, Chong He[✉], *Member, IEEE*,
Shaodan Ma[✉], *Senior Member, IEEE*, and Wen Chen[✉], *Senior Member, IEEE*

Abstract—In this paper, we study an intelligent reflecting surface (IRS)-aided radar-communication (Radcom) system, where the IRS is leveraged to help Radcom base station (BS) transmit the joint of communication signals and radar signals for serving communication users and tracking targets simultaneously. The objective of this paper is to minimize the total transmit power at the Radcom BS by jointly optimizing the active beamformers, including communication beamformers and radar beamformers, at the Radcom BS and the phase shifts at the IRS, subject to the minimum signal-to-interference-plus-noise ratio (SINR) required by communication users, the minimum SINR required by the radar, and the cross-correlation pattern design. In particular, we consider two cases, namely, case I and case II, based on the presence or absence of the radar cross-correlation design and the interference introduced by the IRS on the Radcom BS. For case I where the cross-correlation design and the interference are not considered, we prove that the dedicated radar signals are not needed, which significantly reduces implementation complexity and simplifies algorithm design. Then, a penalty-based algorithm is proposed to solve the resulting non-convex optimization problem. Whereas for case II considering the cross-correlation design and the interference, we unveil that the dedicated radar signals are needed in general to enhance the system performance. Since the resulting optimization problem is more challenging to solve as compared with the case I, the semidefinite relaxation (SDR) based alternating optimization (AO) algorithm is proposed. Particularly, instead of relying on the Gaussian randomization technique to obtain an approximate solution by reconstructing rank-one solution, the tightness is

achieved by our proposed reconstruction strategy. Simulation results demonstrate the effectiveness of proposed algorithms and also show the superiority of the proposed scheme over various benchmark schemes.

Index Terms—Intelligent reflecting surface, passive beamforming, transmit beamforming, integrated sensing and communication.

I. INTRODUCTION

THE rapid increase of mobile data and Internet of Things (IoT) devices are creating unprecedented challenges for wireless service providers to provide high data rate and ultra-reliable low latency communication due to the limited frequency spectrum from 700 MHz and 2.6 GHz in the existing communication networks [1]. In contrast, the radar system has fruitful spectrum resource and typically operate ranging from 0.3-100 GHz, such as S band (2-4 GHz), C band (4-8 GHz), and X band (8-12.5 GHz), depending on specific application requirements [2]. The coexistence (or spectrum sharing) design between the radar system and the wireless communication system is attracting great attention, which allows the communication system to use the spectrum resource of the radar system [3]. To mitigate the interference between the above two systems, several promising approaches are proposed, such as the opportunistic spectrum sharing approach [4], the null-space projection based approach [5], [6], and the joint design of radar waveform and communication beamforming [7], [8]. However, such separated deployment, i.e., the radar transceiver and the communication transmitter are geographically separated, requires additional information, such as the channel state information (CSI), radar probing waveforms, and communication modulation format, etc., to exchange to coordinate the simultaneous radar and communication transmissions, which significantly increases the complexity for hardware implementation in practice.

The radar-communication (Radcom) system (also known as the dual-function radar-communication system [9], [10], [11]), which integrates the radar and communication functions into a single hardware platform and is regarded as a promising solution to simplify the system design [12]. The RadCom system is able to simultaneously perform both radar and communication functionalities using the same signals transmitted from a fully-shared transmitter, which does not require to exchange information and naturally achieves full cooperation. In the early stage, the information is embedded into the radar pulses so that the communication transmission can be readily realized by using the already fabricated radar platforms. For

Manuscript received 22 March 2022; revised 15 June 2022 and 1 August 2022; accepted 21 September 2022. Date of publication 6 October 2022; date of current version 11 April 2023. The work of Meng Hua was supported by the under Grant UMMTP-2020-02. The work of Qingqing Wu was supported in part by the FDCT under Grant 0119/2020/A3 and Grant SKL-IOTSC(UM)-2021-2023 and in part by the GDST under Grant 2021A1515011900 and Grant 2020B1212030003. The work of Shaodan Ma was supported in part by the Science and Technology Development Fund, Macau SAR under Grant 0051/2022/A1, Grant 0036/2019/A1, and Grant SKL-IOTSC(UM)-2021-2023; and in part by the Research Committee of University of Macau under Grant MYRG2020-00095-FST. The work of Wen Chen was supported in part by the National Key Project under Grant 2020YFB1807700 and Grant 2018YFB1801102; in part by the Shanghai Kewei under Grant 20JC1416502 and Grant 22JC1404000; and in part by the NSFC under Grant 62071296. The associate editor coordinating the review of this article and approving it for publication was A. Liu. (*Corresponding author: Qingqing Wu.*)

Meng Hua, Qingqing Wu, and Shaodan Ma are with the State Key Laboratory of Internet of Things for Smart City, University of Macau, Macau (e-mail: menghua@um.edu.mo; qingqingwu@um.edu.mo; shaodanma@um.edu.mo).

Chong He and Wen Chen are with the Department of Electronic Engineering, Shanghai Institute of Advanced Communications and Data Sciences, Shanghai Jiao Tong University, Minhang, Shanghai 200240, China (e-mail: hechong@sjtu.edu.cn; wenchen@sjtu.edu.cn).

Color versions of one or more figures in this article are available at <https://doi.org/10.1109/TWC.2022.3210532>.

Digital Object Identifier 10.1109/TWC.2022.3210532

1536-1276 © 2022 IEEE. Personal use is permitted, but republication/redistribution requires IEEE permission.

See <https://www.ieee.org/publications/rights/index.html> for more information.

example, the communication symbols embedding into radar pulses and/or sidelobe can be realized by controlling the radar pulse's amplitude, phase shift, and even index modulation [13], [14], [15]. However, such approaches result in a low data rate for transmission since the transmission rate is fundamentally constrained by the radar pulse repetition frequency. Another important paradigm of research in existing works on Radcom is the transmit beamforming design [5], [16], [17]. Compared to the information embedding approaches, the transmit beamforming design potentially supports high data rate and guarantees radar performance by synthesizing a joint waveform that is shared by both radar and communications. The seminal work in [5] analyzed the synthesized waveform performance in the shared deployment system, and showed that the shared deployment significantly outperforms than the separated deployment in terms of the trade-off between the radar beampattern synthesis and the quality of communication. Instead of using the synthesized waveforms, the authors in [18] proposed to transmit the combination signals with communication beamformers and radar waveforms at the Radcom base station (BS), where the communication beamformers are used for serving communication users and radar waveforms are used for radar sensing, which provides more degrees of freedom for system design. The results in [18] showed that the communication-only beamformer design is inferior to the joint design of communication beamformer and radar waveform in terms of beampattern synthesis, especially when the number of communication users is less than the number of targets. The authors in [19] further answered whether radar waveforms are needed under different design criteria, channel conditions, and receiver types. However, the above works focused on either the beamforming/waveform design or encoding design, the limited degrees of freedom such as the uncontrollable of electromagnetic waves propagation still confine the system performance.

Recently, intelligent reflecting surfaces (IRSs) attract great attention both from industry and academia [20], [21], [22].¹ The IRS is composed of large numbers of passive and low-cost reflecting elements, each of which is able to independently adjust phase shift and/or amplitude on the impinging electromagnetic signals, so that it is able to controllably change the electromagnetic waves propagation towards any directions of interest. The seminal work in [26] unveiled the fundamental scaling law of the IRS by showing that the received signal-to-noise (SNR) is quadratically increasing with the number of IRS reflecting elements, which was further proved to be applicable for the IRS with even low-resolution phase shifts (e.g., 1-bit resolution) [27]. Based on this appealing result, the IRS has been exploited for different applications such as wireless information transmission [28], [29], [30], [31], [32], wireless-powered communication network [33], [34], [35], unmanned aerial vehicle communication [36], [37], [38],

[39], and non-orthogonal multiple access [40], [41], [42], etc. To unleash the full potential of the Radcom system for both communication and radar sensing, the integration of IRS in the Radcom system is also ongoing. A handful of works, see e.g., [43], [44], [45], [46], [47], studied the IRS used for sensing and two sensing architectures were proposed, namely the fully-passive IRS-aided sensing architecture [43], [44], [45], [46] and the IRS-self-sensing architecture [47]. Some further works, see, e.g., [48], [49], [50], [51], focused on the Radcom system by exploiting IRS to enhance the sensing performance while satisfying the quality-of-service (QoS) of users. The authors in [48] and [49] studied one communication user scenario. To be specific, work [48] studied one target sensing and aimed at maximizing the radar SNR while guaranteeing the QoS of the user by the joint optimization of IRS phase shifts and transmit covariance matrix. In [49], the authors studied the scenario where the BS and multiple sensing targets are blocked and constructed a virtual line-of-sight (LoS) link between the IRS and targets for target sensing. The authors in [50] and [51] further studied the joint design of the active beamforming and the passive beamforming for the multi-user scenario in RIS-assisted Radcom system. The minimization of multi-user interference under the predefined beampattern constraint was studied in [50]. The authors in [51] studied the scenario that the target sensing is corrupted by multiple clutters with the signal-dependent interference and aimed to maximize the radar SINR. However, the above works ignore the impact of interference introduced by the IRS and radar cross-correlation on the system. In addition, regarding the transceiver design for the joint waveform design or the single waveform design is also not answered and studied.

To address the above challenges, this paper studies an IRS-aided Radcom system in multi-user and multi-target scenarios as shown in Fig. 1. Based on the presence or absence of the radar cross-correlation design and the interference introduced by the IRS on the Radcom BS, two cases, namely, case I and case II, are studied. In particular, we answer the fundamental question: whether the dedicated radar signals are needed for these two cases? The main contributions of this paper are summarized as follows.

- We study an IRS-aided Radcom system, where the IRS is leveraged to help the Radcom BS transmit the joint of communication signals and radar signals for serving communication users and tracking targets. Our objective is to minimize the total transmit power at the Radcom BS by jointly optimizing the active beamformers at the Radcom BS and the phase shifts at the IRS, subject to the minimum signal-to-interference-plus-noise ratio (SINR) required by communication users, the minimum SINR required by the radar, and the cross-correlation pattern design. In particular, we consider two cases, i.e., case I and case II, based on the presence or absence of the radar cross-correlation design and the interference introduced by the IRS on the Radcom BS, which results in two different optimization problems.
- For case I where the interference introduced by the IRS is perfectly canceled and the cross-correlation design is ignored. Since the resulting optimization problem is

¹We note that simultaneously transmitting and reflecting (STAR) IRSs not only reflect signals but also refract signals [23], [24], [25], which achieve 360° coverage. Since both paradigms have similar implement principles, our proposed algorithms for the IRS are also applicable to the STAR-IRS with only slight modifications. As such, we consider the IRS having reflecting function in this paper without compromising contributions.

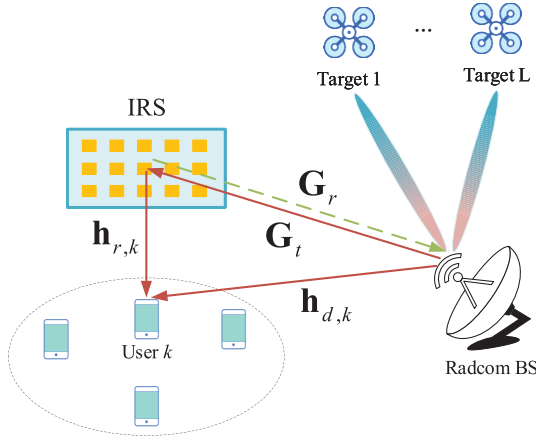


Fig. 1. An IRS-aided radcom system.

non-convex, there are no standard convex methods to solve it optimally. To solve the problem, we first rigorously prove that dedicated radar signals are not needed in this case under the assumptions that complex amplitudes of targets are independently distributed as well as the amplitudes of targets and user channels are uncorrelated, which significantly reduces implementation complexity and simplifies the subsequent algorithm design. Then, we propose a novel penalty-based algorithm, which includes a two-layer iteration, i.e., an inner layer iteration and an outer layer iteration. The inner layer solves the penalized optimization problem, while the outer layer updates the penalty coefficient over iterations to guarantee convergence. In particular, the solution to each subproblem in the inner layer is solved by either a closed-form expression or a semi-closed-form expression.

- For case II where both the cross-correlation pattern design and the interference introduced by the IRS are considered. Since the resulting optimization problem is more challenging to solve than case I, the proposed penalty-based algorithm in case I cannot be applicable to this case. To solve this difficulty, a semidefinite relaxation (SDR)-based alternating optimization (AO) is proposed. In particular, instead of relying on the Gaussian randomization technique to obtain an approximation solution, the tightness is achieved by our proposed reconstruction strategy. In addition, we unveil that the dedicated radar signals are needed in general for this case to enhance the system performance.
- Our simulation results demonstrate that the IRS is beneficial for reducing the transmit power required by the Radcom BS in case I. In addition, it is shown that in case II, as the IRS is deployed far from the Radcom BS, the IRS is helpful for reducing transmit power, while as the IRS is deployed in the vicinity of the Radcom BS, the IRS may even deteriorate the system performance due to the interference. Furthermore, the results also show that adopting dedicated radar signals at the Radcom BS can significantly reduce the system outage probability as compared to the case without adopting the dedicated radar signals in case II.

The rest of this paper is organized as follows. Section II introduces the system model and problem formulation for the considered IRS-aided Radcom system. In Section III, a penalty-based algorithm is proposed to solve case I. In Section IV, an SDR-based AO algorithm is proposed to solve case II. Numerical results are provided in Section V and the paper is concluded in Section VI.

Notations: Boldface upper-case and lower-case letter denote matrix and vector, respectively. $\mathbb{C}^{d_1 \times d_2}$ stands for the set of complex $d_1 \times d_2$ matrices. For a scalar value x , $|x|$ represents the Euclidean norm of x . For a vector \mathbf{x} , \mathbf{x}^* and \mathbf{x}^H stand for its conjugate and conjugate transpose, respectively, and $\text{diag}(\mathbf{x})$ denotes a diagonal matrix whose main diagonal elements are extracted from vector \mathbf{x} . For a matrix \mathbf{X} , $\text{Tr}(\mathbf{X})$ and $\text{rank}(\mathbf{X})$ stand for its trace and rank, respectively, while $\mathbf{X} \succeq \mathbf{0}$ indicates that matrix \mathbf{X} is positive semi-definite. A circularly symmetric complex Gaussian random vector \mathbf{x} with mean $\boldsymbol{\mu}$ and covariance matrix $\boldsymbol{\Sigma}$ is denoted by $\mathbf{x} \sim \mathcal{CN}(\boldsymbol{\mu}, \boldsymbol{\Sigma})$. $\mathbb{E}(\cdot)$ denotes the expectation operation. $\mathcal{O}(\cdot)$ is the big-O computational complexity notation.

II. SYSTEM MODEL AND PROBLEM FORMULATION

A. System Model

Consider an IRS-aided Radcom system consisting of a Radcom BS, K single-antenna users with the set denoted by $\mathcal{K} = \{1, \dots, K\}$, L radar targets with the set denoted by $\mathcal{L} = \{1, \dots, L\}$, and an IRS with M reflecting elements and with the set denoted by $\mathcal{M} = \{1, \dots, M\}$, as shown in Fig. 1.² Following [5], we consider the shared antenna deployment strategy for simultaneously serving communication users and tracking targets since it is superior than the separated antenna deployment strategy in terms of sensing quality and communication quality. The Radcom BS is equipped with $N_t + N_r$ antennas, of which N_t transmit antennas are used for serving communication users and tracking radar targets at the same time ($N_t \geq K$), while N_r receive antennas are dedicated to receiving the echo signals reflected by radar targets.

1) *Transmit Waveform Design:* The transmitted signal by the Radcom BS is given by

$$\mathbf{s} = \mathbf{W}_c \mathbf{x}_c + \mathbf{W}_r \mathbf{x}_r, \quad (1)$$

where $\mathbf{x}_c \in \mathbb{C}^{K \times 1}$ denotes the transmit signals intended for communication users satisfying $\mathbf{x}_c \sim \mathcal{CN}(\mathbf{0}, \mathbf{I}_K)$ and $\mathbf{W}_c \in \mathbb{C}^{N_t \times K}$ represents the corresponding communication beamformer. Similarly, $\mathbf{x}_r \in \mathbb{C}^{N_t \times 1}$ denotes N_t individual radar signals satisfying $\mathbb{E}\{\mathbf{x}_r\} = \mathbf{0}_{N_t \times 1}$ and $\mathbb{E}\{\mathbf{x}_r \mathbf{x}_r^H\} = \mathbf{I}_{N_t}$, and $\mathbf{W}_r \in \mathbb{C}^{N_t \times N_t}$ represents the radar beamformer. In addition, we assume that the communication and radar signals are statistically independent and uncorrelated, i.e., $\mathbb{E}\{\mathbf{x}_c \mathbf{x}_r^H\} = \mathbf{0}_{K \times N_t}$ [18].

2) *Communication Model:* We consider a quasi-static flat-fading channel in which the CSI remains unchanged in a channel coherence block, but may change in the subsequent blocks. We assume that the perfect CSI of all involved channels for

²Although the system considers a single IRS, it can be readily extended to the case with multiple IRSs. In addition, the proposed algorithms in this paper are also applicable to the multiple IRSs case without any modifications.

communication is available at the Radcom BS via sending pilot signals by users [21], [52]. Without loss of generality, in the downlink transmission, denote by $\mathbf{G}_t \in \mathbb{C}^{M \times N_t}$, $\mathbf{h}_{r,k}^H \in \mathbb{C}^{1 \times M}$, and $\mathbf{h}_{d,k}^H \in \mathbb{C}^{1 \times N_t}$ the complex equivalent baseband channel between the Radcom BS and the IRS, between the IRS and the k th user, and between the Radcom BS and the k th user, $k \in \mathcal{K}$, respectively. In addition, denote by $\mathbf{G}_r \in \mathbb{C}^{N_r \times M}$ the complex equivalent baseband channel between the Radcom BS and the IRS in the uplink transmission. The received signal by user k in the downlink is given by

$$y_k = (\mathbf{h}_{d,k}^H + \mathbf{h}_{r,k}^H \mathbf{\Theta} \mathbf{G}_t) \mathbf{s} + n_k, \quad (2)$$

where $\mathbf{\Theta} = \text{diag}(v_1, \dots, v_M)$ represents the IRS reflection coefficient matrix and v_m denotes the phase shift corresponding to the m th IRS reflecting element with $|v_m| = 1$, and $n_k \sim \mathcal{CN}(0, \sigma^2)$ stands for the additive white Gaussian noise at user k . Define $\mathbf{W}_c = [\mathbf{w}_{c,1}, \dots, \mathbf{w}_{c,K}]$, where $\mathbf{w}_{c,k} \in \mathbb{C}^{N_t \times 1}$ denotes the k th column vector of \mathbf{W}_c , $k \in \mathcal{K}$. Similarly, define $\mathbf{W}_r = [\mathbf{w}_{r,1}, \dots, \mathbf{w}_{r,N_t}]$, where $\mathbf{w}_{r,i} \in \mathbb{C}^{N_t \times 1}$ denotes the i th column vector of \mathbf{W}_r , $i \in \mathcal{N}_t = \{1, \dots, N_t\}$. As such, the received SINR by user k is given by

$$\text{SINR}_k = \frac{|\mathbf{h}_k^H \mathbf{w}_{c,k}|^2}{\sum_{i \neq k} |\mathbf{h}_k^H \mathbf{w}_{c,i}|^2 + \sum_{j=1}^{N_t} |\mathbf{h}_k^H \mathbf{w}_{r,j}|^2 + \sigma^2}, \quad k \in \mathcal{K}, \quad (3)$$

where $\mathbf{h}_k^H = \mathbf{h}_{d,k}^H + \mathbf{h}_{r,k}^H \mathbf{\Theta} \mathbf{G}_t$.

3) *Radar Model*: Under the assumption that the propagation is nondispersive for tracking targets, the signal at the l th target location with angle θ_l , $l \in \mathcal{L}$, can be described as $\mathbf{a}_t^H(\theta_l) \mathbf{s}$, where $\mathbf{a}_t^H(\theta) \in \mathbb{C}^{1 \times N_t} = [1, e^{-j2\pi d \sin(\theta)/\lambda}, \dots, e^{-j2\pi d(N_t-1) \sin(\theta)/\lambda}]$ stands for the transmit steering vector at direction θ with d denoting the antenna spacing and λ denoting the carrier wavelength. The received echo signals at the Radcom BS comes from four aspects, i.e., radar-target-radar channel, radar-IRS-radar channel, radar-IRS-target-radar channel, and radar-target-IRS-radar channel. However, [43] showed by both theoretical analysis and numerical simulations that the signals go through the radar-target-IRS-radar channel and radar-IRS-target-radar channel are highly attenuated due to three-hop transmissions, which has little impact on the system performance improvement. Thus, we only need to consider the former two types of echo signals and the received echo signals at the Radcom BS is given by

$$\mathbf{y}_r = \underbrace{\sum_{l=1}^L \beta_l \mathbf{a}_r(\theta_l) \mathbf{a}_t^H(\theta_l) \mathbf{s}}_{\text{reflected by targets}} + \underbrace{\mathbf{G}_r \mathbf{\Theta} \mathbf{G}_t \mathbf{s}}_{\text{reflected by the IRS}} + \mathbf{n}_r, \quad (4)$$

where β_l represents the reflection coefficient of the l th target, which is proportional to the radar-cross section (RCS) of the

l th target³ and $\mathbf{n}_r \sim \mathcal{CN}(\mathbf{0}, \sigma^2 \mathbf{I}_{N_r})$ stands for the additive white Gaussian noise at the Radcom BS. In addition, similar to $\mathbf{a}_t^H(\theta)$, $\mathbf{a}_r(\theta) \in \mathbb{C}^{N_r \times 1}$ denotes the receive steering vector at direction θ . Here, two key points need to be highlighted. First, the communication signals, i.e., $\mathbf{W}_c \mathbf{x}_c$, are not interference for target tracking in the Radcom system (in other words, the communication signals are not only used for downlink communication but also used for target tracking) since the communication signals are known at the Radcom BS. Second, since the reflected signals by IRS in (4) do not contain any information about the targets' information, the radar SINR can be expressed as [8], [56]⁴

$$\text{SINR}_r = \text{tr}(\mathbf{A} \mathbf{R} \mathbf{A}^H (\mathbf{B} \mathbf{R} \mathbf{B}^H + \sigma^2 \mathbf{I}_{N_r})^{-1}), \quad (5)$$

where $\mathbf{R} = \sum_{k=1}^K \mathbf{w}_{c,k} \mathbf{w}_{c,k}^H + \sum_{i=1}^{N_t} \mathbf{w}_{r,i} \mathbf{w}_{r,i}^H$, $\mathbf{A} = \sum_{l=1}^L \beta_l \mathbf{a}_r(\theta_l) \mathbf{a}_t^H(\theta_l)$, and $\mathbf{B} = \mathbf{G}_r \mathbf{\Theta} \mathbf{G}_t$.

B. Problem Formulation

The objective of this paper is to minimize the total transmit power at the Radcom BS by jointly optimizing the active beamformers at the Radcom BS and the phase shifts at the IRS, subject to the minimum SINR required by communication users, the minimum SINR required by radar, and cross-correlation pattern design. Accordingly, the optimization problem is formulated as

$$\min_{\{v_m\}, \{\mathbf{w}_{c,i}\}, \{\mathbf{w}_{r,i}\}} \sum_{k=1}^K \|\mathbf{w}_{c,k}\|^2 + \sum_{i=1}^{N_t} \|\mathbf{w}_{r,i}\|^2 \quad (6a)$$

$$\text{s.t.} \quad \frac{|\mathbf{h}_k^H \mathbf{w}_{c,k}|^2}{\sum_{i \neq k} |\mathbf{h}_k^H \mathbf{w}_{c,i}|^2 + \sum_{i=1}^{N_t} |\mathbf{h}_k^H \mathbf{w}_{r,i}|^2 + \sigma^2} \geq r_{k,\text{th}}, \quad k \in \mathcal{K}, \quad (6b)$$

$$\text{tr}(\mathbf{A} \mathbf{R} \mathbf{A}^H (\mathbf{B} \mathbf{R} \mathbf{B}^H + \sigma^2 \mathbf{I}_{N_r})^{-1}) \geq r_{r,\text{th}}, \quad (6c)$$

$$\sum_{l=1}^{L-1} \sum_{j=l+1}^L |\mathbf{a}_t^H(\theta_l) \mathbf{R} \mathbf{a}_t(\theta_j)|^2 \leq \epsilon_{\text{th}}, \quad (6d)$$

$$|v_m| = 1, \quad m \in \mathcal{M}, \quad (6e)$$

where constraint (6b) denotes the minimum SINR, i.e., $r_{k,\text{th}}$, required by user k , $k \in \mathcal{K}$; constraint (6c) represents that the

³As stated in [53], the target is in general composed of an infinite number of random, isotropic and independent scatterers over the area of interest, and the complex gain of the scatterer can be modeled as a zero-mean and white complex random variable. Together with the fact that incident angles between different targets are randomly distributed, the amplitudes of different targets can thus be assumed to be independently distributed, i.e., $\beta_l \sim \mathcal{CN}(0, \sigma_\beta^2)$ [54], [55].

⁴As stated in [57], maximizing the radar SINR of the received signals is a more justifiable goal than maximizing the total spatial power at a number of given target locations. Thus, we consider the radar SINR as the design metric in this paper. In addition, since maximizing the radar SINR potentially increases the total spatial power at a number of given target locations, the performance of radar tracking is characterized by the transmit beam pattern in the simulations. Furthermore, we assume that targets' locations θ_l , $l \in \mathcal{L}$ and amplitudes of channels β_l , $l \in \mathcal{L}$ are known at the Radcom BS for radar tracking by applying the effective estimation techniques such as generalized likelihood ratio test (GLRT) and Capon methods [17], [58], [59].

received radar SINR should exceed the minimum threshold $r_{r,\text{th}}$; constraint (6d) denotes that the cross-correlation pattern between the probing signals at a number of given target locations must be smaller than ϵ_{th} ; constraint (6e) denotes the unit-modulus constraint on each IRS reflection coefficient. Note that the cross-correlation constraint is introduced here to ensure that the signals reflected by the targets are independent of each other so that the adaptive radar multiple-input multiple-output (MIMO) techniques can be used for detection and tracking.

Problem (6) is non-convex since the optimization variables are highly coupled in constraints (6b)-(6d) and the unit-modulus constraint is imposed on each reflection coefficient v_m in (6e), there are no standard methods for solving such non-convex optimization problem optimally in general. In the following, we further study two cases, namely, case I and case II, based on the presence or absence of the cross-correlation pattern constraint (6d) and the interference introduced by the IRS in Section III and Section IV, and then propose two algorithms, namely, a penalty-based algorithm and an SDR-based algorithm, to solve them, respectively.

III. PROPOSED SOLUTION TO CASE I

In this section, we study problem (6) by assuming that the interference introduced by the IRS, i.e., $\mathbf{G}_r \Theta \mathbf{G}_t \mathbf{s}$ in (4), is perfectly canceled at the Radcom BS and ignoring the cross-correlation pattern design. Thus, the radar SINR in (5) is reduced to $\text{SINR}_r = \text{tr}(\mathbf{A} \mathbf{R} \mathbf{A}^H) / \sigma^2 = \left(\sum_{k=1}^K \mathbf{w}_{c,k}^H \mathbf{A}^H \mathbf{A} \mathbf{w}_{c,k} + \sum_{i=1}^{N_t} \mathbf{w}_{r,i}^H \mathbf{A}^H \mathbf{A} \mathbf{w}_{r,i} \right) / \sigma^2$. Accordingly, problem (6) can be simplified to

$$\min_{\{v_m\}, \{\mathbf{w}_{c,i}\}, \{\mathbf{w}_{r,i}\}} \sum_{k=1}^K \|\mathbf{w}_{c,k}\|^2 + \sum_{i=1}^{N_t} \|\mathbf{w}_{r,i}\|^2 \quad (7a)$$

$$\text{s.t.} \quad \sum_{k=1}^K \mathbf{w}_{c,k}^H \mathbf{A}^H \mathbf{A} \mathbf{w}_{c,k} + \sum_{i=1}^{N_t} \mathbf{w}_{r,i}^H \mathbf{A}^H \mathbf{A} \mathbf{w}_{r,i} \geq r_{r,\text{th}} \sigma^2, \quad (7b)$$

$$(6b), (6e). \quad (7c)$$

It is not difficult to check that problem (7) is non-convex. In the following, we first exploit the hidden structure of problem (7) and derive the following theorem:

Theorem 1: Under the assumptions of independently distributed complex amplitudes of targets, i.e., the non-zero singular values of $\mathbf{A}^H \mathbf{A}$ are not same, and amplitudes of targets and user channels are uncorrelated, the optimal solution of problem (7) satisfies $\mathbf{w}_{r,i}^{\text{opt}} = \mathbf{0}$, $i \in \mathcal{N}_t$.

Proof: Please refer to Appendix A. ■

Theorem 1 indicates that the dedicated radar beams, i.e., $\{\mathbf{w}_{r,i}, i \in \mathcal{N}_t\}$, are not needed for achieving the minimum Radcom BS transmit power. This can be intuitively understood since sending dedicated radar signals not only consumes transmit power but also potentially causes interference to communication users. Based on Theorem 1, the implementation complexity of the Radcom BS as well as the algorithm design is reduced.

To obtain a high-quality solution, a penalty-based algorithm is proposed to decouple the constraint coupling between the variables in different blocks. Specifically, we first introduce several auxiliary variables $\{x_{k,i}^c, \mathbf{y}_i^c, k \in \mathcal{K}, i \in \mathcal{K}\}$, and define $\mathbf{h}_k^H \mathbf{w}_{c,i} = x_{k,i}^c$ and $\mathbf{A} \mathbf{w}_{c,i} = \mathbf{y}_i^c$, $k \in \mathcal{K}, i \in \mathcal{K}$, problem (7) (by dropping radar beams) can be rewritten as

$$\min_{\{v_m\}, \{\mathbf{w}_{c,i}\}, \{x_{k,i}^c, \mathbf{y}_i^c\}} \sum_{k=1}^K \|\mathbf{w}_{c,k}\|^2 \quad (8a)$$

$$\text{s.t.} \quad \frac{|x_{k,k}^c|^2}{\sum_{i \neq k} |x_{k,i}^c|^2 + \sigma^2} \geq r_{k,\text{th}}, k \in \mathcal{K}, \quad (8b)$$

$$\sum_{i=1}^K \|\mathbf{y}_i^c\|^2 \geq \sigma^2 r_{r,\text{th}}, \quad (8c)$$

$$\mathbf{h}_k^H \mathbf{w}_{c,i} = x_{k,i}^c, \mathbf{A} \mathbf{w}_{c,i} = \mathbf{y}_i^c, i \in \mathcal{K}, k \in \mathcal{K}, \quad (8d)$$

$$(6e). \quad (8e)$$

It can be seen that the optimization variables in constraints (8b) and (8c) are fully decoupled since these two constraints do not contain any common optimization variables. We then use (8d) as penalty terms that are added to the objective function (8a), yielding the following penalty-based optimization problem

$$\min_{\{v_m\}, \{\mathbf{w}_{c,i}\}, \{x_{k,i}^c, \mathbf{y}_i^c\}} \sum_{k=1}^K \|\mathbf{w}_{c,k}\|^2 + \frac{1}{2\rho} \left(\sum_{k=1}^K \sum_{i=1}^K |\mathbf{h}_k^H \mathbf{w}_{c,i} - x_{k,i}^c|^2 + \sum_{i=1}^K \|\mathbf{A} \mathbf{w}_{c,i} - \mathbf{y}_i^c\|^2 \right) \quad (9a)$$

$$\text{s.t.} \quad (6e), (8b), (8c). \quad (9b)$$

where ρ ($\rho > 0$) represents the penalty coefficient used to penalize the violation of the equality in constraint (8d). By gradually decreasing the value of ρ over outer layer iterations, as $\rho \rightarrow 0$, it follows that $1/(2\rho) \rightarrow \infty$. As such, the equality in (8d) is guaranteed by the optimal solution to problem (9). With fixed ρ , it can be seen that problem (9) is still non-convex. To tackle this non-convex optimization problem, we divide all the optimization variables into three blocks in the inner layer, namely, 1) transmit beamformers $\{\mathbf{w}_{c,i}\}$, 2) IRS phase shifts $\{v_m\}$, and 3) auxiliary variables $\{x_{k,i}^c, \mathbf{y}_i^c\}$, and then alternately optimize each block, until convergence is achieved.

A. Inner Layer Optimization

In this subsection, we elaborate on how to solve the above three subproblems. In particular, we obtain a closed-form and/or a semi-closed-form solution to each of these three subproblems.

1) For Any Given Phase Shifts $\{v_m\}$ and Auxiliary Variables $\{x_{k,i}^c, \mathbf{y}_i^c\}$, the Subproblem Corresponding to the Trans-

mit Beamformer Optimization Is Given by:

$$\min_{\{\mathbf{w}_{c,i}\}} \sum_{k=1}^K \|\mathbf{w}_{c,k}\|^2 + \frac{1}{2\rho} \left(\sum_{k=1}^K \sum_{i=1}^K |\mathbf{h}_k^H \mathbf{w}_{c,i} - x_{k,i}^c|^2 + \sum_{i=1}^K \|\mathbf{A} \mathbf{w}_{c,i} - \mathbf{y}_i^c\|^2 \right) \quad (10)$$

It can be readily observed that problem (10) is a convex quadratic minimization problem without constraints. Thus, we can obtain its optimal solution by exploiting the first-order optimality conditions. Specifically, by taking the first-order derivative of the objective function (10) with respect to (w.r.t.) $\mathbf{w}_{c,i}$ and setting it to zero, the closed-form solution of $\mathbf{w}_{c,i}$ can be obtained as

$$\mathbf{w}_{c,i}^{\text{opt}} = \frac{1}{2\rho} \left(\mathbf{I}_{N_t} + \frac{1}{2\rho} \left(\sum_{k=1}^K \mathbf{h}_k \mathbf{h}_k^H + \mathbf{A}^H \mathbf{A} \right) \right)^{-1} \times \left(\sum_{k=1}^K \mathbf{h}_k x_{k,i}^c + \mathbf{A}^H \mathbf{y}_i^c \right), \quad i \in \mathcal{K}. \quad (11)$$

2) For Any Given Transmit Beamformers $\{\mathbf{w}_{c,i}\}$ and Auxiliary Variables $\{x_{k,i}^c, \mathbf{y}_i^c\}$, the Subproblem Corresponding to the IRS Phase-Shift Optimization Is Given by (by Dropping Constants ρ , $\|\mathbf{w}_{c,i}\|^2$'s, and $\|\mathbf{A} \mathbf{w}_{c,i} - \mathbf{y}_i^c\|^2$'s):

$$\min_{\{v_m\}} \sum_{k=1}^K \sum_{i=1}^K |\mathbf{h}_k^H \mathbf{w}_{c,i} - x_{k,i}^c|^2 \quad (12a)$$

$$\text{s.t. (6e).} \quad (12b)$$

Recall that $\mathbf{h}_k^H = \mathbf{h}_{d,k}^H + \mathbf{h}_{r,k}^H \Theta \mathbf{G}_t$, $k \in \mathcal{K}$, it is not difficult to verify that objective function (12a) is a convex quadratic function. However, due to the unit-modulus constraint on each IRS phase shift in (6e), problem (12) is a non-convex optimization problem. To solve this problem, an element-wise algorithm is proposed, where the main idea behind it is to optimize one phase shift with the other phase shifts are fixed. Specifically, we rewrite $\mathbf{h}_k^H = \mathbf{h}_{d,k}^H + \mathbf{h}_{r,k}^H \Theta \mathbf{G}_t$ as

$$\mathbf{h}_k^H = \mathbf{h}_{d,k}^H + \mathbf{v}^H \text{diag}(\mathbf{h}_{r,k}^H) \mathbf{G}_t, \quad k \in \mathcal{K}, \quad (13)$$

where $\mathbf{v}^H = [v_1, \dots, v_M]$. Then, define $\mathbf{q}_{k,i}^c = \text{diag}(\mathbf{h}_{r,k}^H) \mathbf{G}_t \mathbf{w}_{c,i}$, $k \in \mathcal{K}, i \in \mathcal{K}$, we can write $|\mathbf{h}_k^H \mathbf{w}_{c,i} - x_{k,i}^c|^2$ w.r.t. the m th IRS phase shift, i.e., v_m , in a more compact form given by

$$|\mathbf{h}_k^H \mathbf{w}_{c,i} - x_{k,i}^c|^2 \stackrel{(a)}{=} \left| [\mathbf{q}_{k,i}^c]_m \right|^2 + 2\text{Re} \left\{ v_m [\mathbf{q}_{k,i}^c]_m a_{k,i,\bar{m}}^{c,H} \right\} + |a_{k,i,\bar{m}}^c|^2, \quad k \in \mathcal{K}, i \in \mathcal{K}, \quad (14)$$

where (a) holds due to $|v_m| = 1, \forall m$, and $a_{k,i,\bar{m}}^c = \sum_{j \neq m}^M v_j [\mathbf{q}_{k,i}^c]_j + \mathbf{h}_{d,k}^H \mathbf{w}_{c,i} - x_{k,i}^c$.

Therefore, problem (12) regarding to the m th IRS phase-shift optimization becomes (by dropping irrelevant constants w.r.t. v_m)

$$\min_{v_m} \text{Re} \left\{ v_m \left(\sum_{k=1}^K \sum_{i=1}^K [\mathbf{q}_{k,i}^c]_m a_{k,i,\bar{m}}^{c,H} \right) \right\} \quad (15a)$$

$$\text{s.t. } |v_m| = 1. \quad (15b)$$

It can be observed that the objective function of problem (15) is linear w.r.t. v_m , and the optimal solution to problem (15) can be obtained as

$$v_m^{\text{opt}} = -\exp \left(j \arg \left(\sum_{k=1}^K \sum_{i=1}^K [\mathbf{q}_{k,i}^c]_m a_{k,i,\bar{m}}^{c,H} \right)^* \right). \quad (16)$$

Based on (16), we can alternately optimize each IRS phase shift in an iterative manner.

3) For Any Given IRS Phase Shifts $\{v_m\}$ and Transmit Beamformers $\{\mathbf{w}_{c,i}\}$, the Auxiliary Variables Can Be Optimized by Solving the Following Subproblem (by Dropping Constants ρ and $\|\mathbf{w}_{c,i}\|^2$'s):

$$\min_{\{x_{k,i}^c, \mathbf{y}_i^c\}} \sum_{k=1}^K \sum_{i=1}^K |\mathbf{h}_k^H \mathbf{w}_{c,i} - x_{k,i}^c|^2 + \sum_{i=1}^K \|\mathbf{A} \mathbf{w}_{c,i} - \mathbf{y}_i^c\|^2 \quad (17a)$$

$$\text{s.t. (8b), (8c).} \quad (17b)$$

Since optimization variables w.r.t. different blocks $\{x_{k,i}^c, i \in \mathcal{K}\}$ for $k \in \mathcal{K}$ and $\{\mathbf{y}_i^c, i \in \mathcal{K}\}$ are separated in both the objective function and constraints. Therefore, problem (17) can be divided into $K+1$ separated subproblems, which can be solved in a parallel manner as follows.

On the one hand, the subproblem regarding to the k th block $\{x_{k,i}^c, i \in \mathcal{K}\}$ is given by

$$\min_{\{x_{k,i}^c\}} \sum_{i=1}^K |\mathbf{h}_k^H \mathbf{w}_{c,i} - x_{k,i}^c|^2 \quad (18a)$$

$$\text{s.t. (8b).} \quad (18b)$$

It is not difficult to see that problem (18) is a quadratically constrained quadratic program (QCQP) problem with convex objective function and non-convex constraint (8b). Fortunately, it was shown in [60, Appendix B.1] that the strong duality holds for any optimization problem with quadratic objective and one quadratic inequality constraint, provided Slater's condition holds. This result shows that the optimal solution to problem (18) can be obtained by solving its dual problem. By introducing dual variable $\lambda_{2,k}$ ($\lambda_{2,k} \geq 0$) associated with constraint (8b), the Lagrangian function of problem (18) is given by

$$\begin{aligned} \mathcal{L}_2(x_{k,i}^c, \lambda_{2,k}) &= \sum_{i=1}^K |\mathbf{h}_k^H \mathbf{w}_{c,i} - x_{k,i}^c|^2 \\ &\quad + \lambda_{2,k} \left(r_{k,\text{th}} \left(\sum_{i \neq k}^K |x_{k,i}^c|^2 + \sigma^2 \right) - |x_{k,k}^c|^2 \right). \end{aligned} \quad (19)$$

Accordingly, the corresponding dual function is given by $f_2(\lambda_{2,k}) = \min_{x_{k,i}^c} \mathcal{L}_2(x_{k,i}^c, \lambda_{2,k})$.

Lemma 2: To make dual function $f_2(\lambda_{2,k})$ bounded, we must have

$$0 \leq \lambda_{2,k} < 1. \quad (20)$$

Proof: Please refer to Appendix B. ■

Based on Lemma 2, the optimal solution to $f_2(\lambda_{2,k})$ can be obtained by leveraging the first-order optimality conditions. Specifically, by taking the first-order derivative of $\mathcal{L}_2(x_{k,i}^c, \lambda_{2,k})$ w.r.t. $x_{k,i}^c$ and setting it to zero, we obtain the optimal solution as

$$x_{k,i}^{c,\text{opt}}(\lambda_{2,k}) = \begin{cases} \frac{\mathbf{h}_k^H \mathbf{w}_{c,i}}{1 + \lambda_{2,k} r_{k,\text{th}}}, & i \neq k, i \in \mathcal{K}, \\ \frac{\mathbf{h}_k^H \mathbf{w}_{c,k}}{1 - \lambda_{2,k}}, & i = k. \end{cases} \quad (21)$$

Recall that for the optimal solutions $x_{k,i}^{c,\text{opt}}(\lambda_{2,k})$ and $\lambda_{2,k}^{\text{opt}}$, the following complementary slackness condition must be satisfied [60]

$$\lambda_{2,k}^{\text{opt}} \left(r_{k,\text{th}} \left(\sum_{i \neq k}^K \left| x_{k,i}^{c,\text{opt}}(\lambda_{2,k}^{\text{opt}}) \right|^2 + \sigma^2 \right) - \left| x_{k,k}^{c,\text{opt}}(\lambda_{2,k}^{\text{opt}}) \right|^2 \right) = 0. \quad (22)$$

Next, we check whether $\lambda_{2,k}^{\text{opt}} = 0$ is the optimal solution or not. If

$$r_{k,\text{th}} \left(\sum_{i \neq k}^K \left| x_{k,i}^{c,\text{opt}}(0) \right|^2 + \sigma^2 \right) - \left| x_{k,k}^{c,\text{opt}}(0) \right|^2 < 0, \quad (23)$$

which indicates that the optimal dual variable $\lambda_{2,k}^{\text{opt}}$ equals to 0, otherwise, the optimal $\lambda_{2,k}^{\text{opt}}$ is a positive value, i.e., $\lambda_{2,k}^{\text{opt}} > 0$, and should satisfy

$$r_{k,\text{th}} \left(\sum_{i \neq k}^K \left| x_{k,i}^{c,\text{opt}}(\lambda_{2,k}^{\text{opt}}) \right|^2 + \sigma^2 \right) - \left| x_{k,k}^{c,\text{opt}}(\lambda_{2,k}^{\text{opt}}) \right|^2 = 0. \quad (24)$$

It can be seen that $\left| x_{k,i}^{c,\text{opt}}(\lambda_{2,k}) \right|$ for $i \neq k$ is monotonically decreasing with $\lambda_{2,k}$, while $\left| x_{k,k}^{c,\text{opt}}(\lambda_{2,k}) \right|$ is monotonically increasing with $\lambda_{2,k}$ for $0 < \lambda_{2,k} < 1$. As such, the optimal $\lambda_{2,k}^{\text{opt}}$ can be obtained by applying a simple bisection search method.

On the other hand, the subproblem regarding to block $\{\mathbf{y}_i^c, i \in \mathcal{K},\}$ is formulated as

$$\min_{\{\mathbf{y}_i^c\}} \sum_{i=1}^K \|\mathbf{A} \mathbf{w}_{c,i} - \mathbf{y}_i^c\|^2 \quad (25a)$$

$$\text{s.t. (8c).} \quad (25b)$$

It can be observed that problem (25) is also a QCQP problem with a quadratic objective and one quadratic inequality constraint. Following [60, Appendix B.1], the strong duality also holds for problem (25). Thus, the optimal solution to problem (25) can be obtained by solving its dual problem. By introducing dual variable λ_3 ($\lambda_3 \geq 0$) associated with constraint (8c), the Lagrangian function of (25) is given by

$$\mathcal{L}_3(\mathbf{y}_i^c, \lambda_3) = \sum_{i=1}^K \|\mathbf{A} \mathbf{w}_{c,i} - \mathbf{y}_i^c\|^2 + \lambda_3 \left(\sigma^2 r_{r,\text{th}} - \sum_{i=1}^K \|\mathbf{y}_i^c\|^2 \right). \quad (26)$$

Let $f_3(\lambda_3) = \min_{\mathbf{y}_i^c} \mathcal{L}_3(\mathbf{y}_i^c, \lambda_3)$ be the dual function of problem (25), we have the following lemma:

Lemma 3: To guarantee the dual function $f_3(\lambda_3)$ be bounded, it follows that

$$0 \leq \lambda_3 < 1. \quad (27)$$

Proof: The proof is similar to Lemma 2 and is omitted here for brevity. ■

Based on Lemma 3, by exploiting the first-order optimality conditions, the optimal solution to $f_3(\lambda_3)$ is given by

$$\mathbf{y}_i^{c,\text{opt}}(\lambda_3) = \frac{\mathbf{A} \mathbf{w}_{c,i}}{1 - \lambda_3}, \quad i \in \mathcal{K}. \quad (28)$$

The optimal dual variable λ_3^{opt} should be chosen for ensuring that the following complementary slackness condition is satisfied:

$$\lambda_3^{\text{opt}} \left(\sigma^2 r_{r,\text{th}} - \sum_{i=1}^K \|\mathbf{y}_i^c(\lambda_3^{\text{opt}})\|^2 \right) = 0. \quad (29)$$

Define $\Gamma(\lambda_3) = \sum_{i=1}^K \|\mathbf{y}_i^c(\lambda_3)\|^2$. Then, substituting (28) into $\Gamma(\lambda_3)$, we have

$$\Gamma(\lambda_3) = \frac{\sum_{i=1}^K \|\mathbf{A} \mathbf{w}_{c,i}\|^2}{(1 - \lambda_3)^2}. \quad (30)$$

It can be observed that $\Gamma(\lambda_3)$ is monotonically increasing with λ_3 for $0 \leq \lambda_3 < 1$. Thus, if $\sigma^2 r_{r,\text{th}} - \Gamma(0) < 0$, which indicates that the optimal dual variable is $\lambda_3^{\text{opt}} = 0$. Otherwise, the optimal λ_3^{opt} can be obtained by solving the following equation:

$$\Gamma(\lambda_3) = \sigma^2 r_{r,\text{th}}. \quad (31)$$

By exploiting the monotonic property of $\Gamma(\lambda_3)$, the solution λ_3^{opt} that satisfies (31) can be readily obtained by applying the simple bisection method searching from 0 to 1.

B. Outer Layer Update

In the outer layer, we need to gradually decrease the penalty coefficient ρ^t in the t th iteration, which can be updated as follow

$$\rho^t = c \rho^{t-1}, \quad (32)$$

where c ($0 < c < 1$) denotes the updated step size. Generally, a larger value of c can achieve better performance but at the cost of more iterations for updating in the outer layer. Although a smaller value of c requires fewer outer layer iterations for updating, the penalty algorithm is more easily diverged. From empirical test, it is promising to choose c from 0.7 to 0.9 to balance the system performance and computational complexity.

C. Overall Algorithm

Next, we provide the termination condition for our proposed algorithm, which is given by

$$\xi = \max \left\{ \left| \mathbf{h}_k^H \mathbf{w}_{c,i} - x_{k,i}^c \right|^2, \|\mathbf{A} \mathbf{w}_{c,i} - \mathbf{y}_i^c\|_\infty^2, i \in \mathcal{K}, k \in \mathcal{K} \right\}, \quad (33)$$

Algorithm 1 Penalty-Based Algorithm for Solving Problem (7)

```

1: Initialize  $\mathbf{v}$ ,  $x_{k,i}^c$ ,  $\mathbf{y}_i^c$ ,  $c$ ,  $\rho^t$ ,  $\varepsilon_1$ , and  $\varepsilon_2$ .
2: repeat: outer layer
3:   repeat: inner layer
4:     Update transmit beamformers  $\{\mathbf{w}_{c,i}\}$  based on (11).
5:     Update IRS phase shifts  $\{v_m\}$  based on (16).
6:     Update  $\{x_{k,i}^c\}$  by solving problem (18).
7:     Update  $\{\mathbf{y}_i^c\}$  by solving problem (25).
8:   until the fractional decrease of the objective value of (9)
      is below a threshold  $\varepsilon_1$ .
9:   Update penalty coefficient  $\rho$  based on (32).
10: until termination indicator  $\xi$  is below a predefined thresh-
      old  $\varepsilon_2$ .

```

where ξ denotes the termination indicator. If ξ is smaller than a predefined value, which indicates that constraint (8d) is met with equality. The details of the proposed penalty-based algorithm are summarized in Algorithm 1.

In Algorithm 1, each block in the inner layer is optimally solved and the objective value of problem (9) is thus non-increasing over iterations in each inner layer. In addition, the optimal objective value of problem (9) is lower-bounded by a finite value due to the minimum SINR required by users. Following [61, Theorem 4.1], the solution obtained by Algorithm 1 is guaranteed to converge to a stationary point.

The computational complexity of Algorithm 1 is calculated as follows. In steps 4 and 5, the closed-form solutions are obtained, whose computational complexity are given by $\mathcal{O}(N_t^3 K)$ and $\mathcal{O}(MN_r^2)$, respectively. In steps 6 and 7, a bisection method is applied, whose computational complexity are given by $\mathcal{O}(K \log_2(\frac{1}{\varepsilon_3}) N_r^2)$ and $\mathcal{O}(\log_2(\frac{1}{\varepsilon_3}) N_r^2)$, respectively, where ε_3 denotes the iteration accuracy. Therefore, the overall complexity of Algorithm 1 is given by $\mathcal{O}(I_{\text{outer}}(I_{\text{inner}}(N_t^3 K + MN_r^2 + (K+1) \log_2(\frac{1}{\varepsilon_3}) N_r^2)))$, where I_{inner} and I_{outer} denote the number of iterations required for convergence in the inner layer and outer layer, respectively.

IV. PROPOSED SOLUTION TO CASE II

In this section, we consider case II where the interference introduced by IRS is uncanceled and the cross-correlation pattern design is required. The penalty-based algorithm proposed in case I is not applicable to this case. To tackle this difficulty, an SDR-based AO algorithm is proposed.

Recall that $\mathbf{Z}_r = \mathbf{W}_r \mathbf{W}_r^H$ and $\mathbf{W}_{c,k} = \mathbf{w}_{c,k} \mathbf{w}_{c,k}^H$ defined in Appendix A, which satisfy $\mathbf{Z}_r \succeq \mathbf{0}$, $\mathbf{W}_{c,k} \succeq \mathbf{0}$, and $\text{rank}(\mathbf{W}_{c,k}) = 1, k \in \mathcal{K}$. We can rewrite \mathbf{R} defined in (5) as $\mathbf{R} = \sum_{k=1}^K \mathbf{W}_{c,k} + \mathbf{Z}_r$. Since the rank-one constraint is non-convex, we apply SDR to relax this constraint. As a result, the SDR of problem (6) is given by

$$\min_{\{v_m\}, \{\mathbf{W}_{c,k}\}, \mathbf{Z}_r} \sum_{k=1}^K \text{tr}(\mathbf{W}_{c,k}) + \text{tr}(\mathbf{Z}_r) \quad (34a)$$

$$\begin{aligned} \text{s.t. } & \mathbf{h}_k^H \left(\sum_{k=1}^K \mathbf{W}_{c,k} + \mathbf{Z}_r \right) \mathbf{h}_k + \sigma^2 \\ & \leq \left(\frac{1}{r_{k,\text{th}}} + 1 \right) \mathbf{h}_k^H \mathbf{W}_{c,k} \mathbf{h}_k, k \in \mathcal{K}, \end{aligned} \quad (34b)$$

$$\begin{aligned} & \text{tr} \left(\mathbf{A} \left(\sum_{k=1}^K \mathbf{W}_{c,k} + \mathbf{Z}_r \right) \mathbf{A}^H \right. \\ & \times \left. \left(\mathbf{B} \left(\sum_{k=1}^K \mathbf{W}_{c,k} + \mathbf{Z}_r \right) \mathbf{B}^H + \sigma^2 \mathbf{I}_{N_r} \right)^{-1} \right) \\ & \geq r_{r,\text{th}}, \end{aligned} \quad (34c)$$

$$\begin{aligned} & \sum_{l=1}^{L-1} \sum_{j=l+1}^L \left| \mathbf{a}_t^H(\theta_l) \left(\sum_{k=1}^K \mathbf{W}_{c,k} + \mathbf{Z}_r \right) \mathbf{a}_t(\theta_j) \right|^2 \\ & \leq \epsilon_{\text{th}}, \end{aligned} \quad (34d)$$

$$(6e). \quad (34e)$$

It is not difficult to verify that constraints (6e), (34b), and (34c) are all non-convex, which in general there are no efficient approaches to solve it optimally. In the following, we first derive the lower bound of constraint (34c) based on the identity

$$\text{tr} \left(\mathbf{A} \mathbf{R} \mathbf{A}^H (\mathbf{B} \mathbf{R} \mathbf{B}^H + \sigma^2 \mathbf{I}_{N_r})^{-1} \right) \geq \frac{\text{tr}(\mathbf{A} \mathbf{R} \mathbf{A}^H)}{\text{tr}(\mathbf{B} \mathbf{R} \mathbf{B}^H + \sigma^2 \mathbf{I}_{N_r})}. \quad (35)$$

As such, constraint (34c) can be approximated as a more tractable form given by

$$\begin{aligned} & \text{tr} \left(\mathbf{A} \left(\sum_{k=1}^K \mathbf{W}_{c,k} + \mathbf{Z}_r \right) \mathbf{A}^H \right) \\ & \geq r_{r,\text{th}} \left(\text{tr} \left(\mathbf{B} \left(\sum_{k=1}^K \mathbf{W}_{c,k} + \mathbf{Z}_r \right) \mathbf{B}^H \right) + \sigma^2 N_r \right). \end{aligned} \quad (36)$$

To tackle the non-convexity of constraint (6e), we relax it as a convex form given by

$$|v_m| \leq 1, \quad m \in \mathcal{M}. \quad (37)$$

Then, we partition all optimization variables into two blocks, i.e., transmit covariance matrices $\{\mathbf{W}_{c,k}, \mathbf{Z}_r\}$ and IRS phase shifts $\{v_m\}$, and optimize these two blocks in an iterative manner.

A. Optimization of Transmit Covariance Matrices

For any given IRS phase shifts $\{v_m\}$, the subproblem regarding to the transmit covariance matrix optimization is given by

$$\min_{\{\mathbf{W}_{c,k}\}, \mathbf{Z}_r} \sum_{k=1}^K \text{tr}(\mathbf{W}_{c,k}) + \text{tr}(\mathbf{Z}_r) \quad (38a)$$

$$\text{s.t. (34b), (34d), (36)}. \quad (38b)$$

It is not difficult to observe that the objective function as well as constraints are all convex, problem (38) is thus convex and can be solved by the interior-point method [60].

B. Optimization of IRS Phase Shifts

For any given transmit covariance matrices $\{\mathbf{W}_{c,k}, \mathbf{Z}_r\}$, the corresponding IRS phase-shift subproblem is given by

$$\text{Find}\{v_m\} \quad (39a)$$

$$\text{s.t. (34b), (36), (37).} \quad (39b)$$

Recall that $\mathbf{h}_k^H = \mathbf{h}_{d,k}^H + \mathbf{v}^H \text{diag}(\mathbf{h}_{r,k}^H) \mathbf{G}_t$, we can expand $\mathbf{h}_k^H \mathbf{R} \mathbf{h}_k$, $k \in \mathcal{K}$, as

$$\begin{aligned} \mathbf{h}_k^H \mathbf{R} \mathbf{h}_k &= \mathbf{h}_{d,k}^H \mathbf{R} \mathbf{h}_{d,k} + 2\text{Re}\{\mathbf{v}^H \text{diag}(\mathbf{h}_{r,k}^H) \mathbf{G}_t \mathbf{R} \mathbf{h}_{d,k}\} \\ &\quad + \mathbf{v}^H \text{diag}(\mathbf{h}_{r,k}^H) \mathbf{G}_t \mathbf{R} \mathbf{G}_t^H \text{diag}(\mathbf{h}_{r,k}) \mathbf{v} \triangleq f_{1,k}(\mathbf{v}). \end{aligned} \quad (40)$$

It is not difficult to see that $f_{1,k}(\mathbf{v})$ is a quadratic function of \mathbf{v} , which is convex.

Similarly, we can rewrite $\mathbf{h}_k^H \mathbf{W}_{c,k} \mathbf{h}_k$, $k \in \mathcal{K}$, as

$$\begin{aligned} \mathbf{h}_k^H \mathbf{W}_{c,k} \mathbf{h}_k &= \mathbf{h}_{d,k}^H \mathbf{W}_{c,k} \mathbf{h}_{d,k} + 2\text{Re}\{\mathbf{v}^H \text{diag}(\mathbf{h}_{r,k}^H) \mathbf{G}_t \mathbf{W}_{c,k} \mathbf{h}_{d,k}\} \\ &\quad + \mathbf{v}^H \text{diag}(\mathbf{h}_{r,k}^H) \mathbf{G}_t \mathbf{W}_{c,k} \mathbf{G}_t^H \text{diag}(\mathbf{h}_{r,k}) \mathbf{v} \triangleq f_{2,k}(\mathbf{v}). \end{aligned} \quad (41)$$

Although $f_{2,k}(\mathbf{v})$ is a quadratic function of \mathbf{v} , the resulting set in (34b) is not a convex set since the super-level set of a convex quadratic function is not convex in general. However, we can linearize $\mathbf{v}^H \text{diag}(\mathbf{h}_{r,k}^H) \mathbf{G}_t \mathbf{W}_{c,k} \mathbf{G}_t^H \text{diag}(\mathbf{h}_{r,k}) \mathbf{v}$ into a linear form by taking its first-order Taylor expansion at any given point \mathbf{v}^t in the t th iteration, yielding the following inequality

$$\begin{aligned} \mathbf{v}^H \text{diag}(\mathbf{h}_{r,k}^H) \mathbf{G}_t \mathbf{W}_{c,k} \mathbf{G}_t^H \text{diag}(\mathbf{h}_{r,k}) \mathbf{v} &\triangleq \bar{f}_{2,k}^{\text{lb}}(\mathbf{v}) \\ &\geq -\mathbf{v}^{t,H} \text{diag}(\mathbf{h}_{r,k}^H) \mathbf{G}_t \mathbf{W}_{c,k} \mathbf{G}_t^H \text{diag}(\mathbf{h}_{r,k}) \mathbf{v}^t \\ &\quad + 2\text{Re}\{\mathbf{v}^{t,H} \text{diag}(\mathbf{h}_{r,k}^H) \mathbf{G}_t \mathbf{W}_{c,k} \mathbf{G}_t^H \text{diag}(\mathbf{h}_{r,k}) \mathbf{v}\}. \end{aligned} \quad (42)$$

As such, the lower bound of $\mathbf{h}_k^H \mathbf{W}_{c,k} \mathbf{h}_k$, denoted by $\bar{f}_{2,k}^{\text{lb}}(\mathbf{v})$, is given by

$$\begin{aligned} \bar{f}_{2,k}^{\text{lb}}(\mathbf{v}) &\triangleq \mathbf{h}_{d,k}^H \mathbf{W}_{c,k} \mathbf{h}_{d,k} \\ &\quad + 2\text{Re}\{\mathbf{v}^H \text{diag}(\mathbf{h}_{r,k}^H) \mathbf{G}_t \mathbf{W}_{c,k} \mathbf{h}_{d,k}\} + \bar{f}_{2,k}^{\text{lb}}(\mathbf{v}), \end{aligned} \quad (43)$$

which is a linear function of \mathbf{v} and thus it is convex.

In addition, recall that $\mathbf{R} = \sum_{k=1}^K \mathbf{W}_{c,k} + \mathbf{Z}_r$ and $\mathbf{B} = \mathbf{G}_r \mathbf{\Theta} \mathbf{G}_t$, we can expand the right-hand side of (36), i.e., $\text{tr}\left(\mathbf{B} \left(\sum_{k=1}^K \mathbf{W}_{c,k} + \mathbf{Z}_r\right) \mathbf{B}^H\right)$, as

$$\begin{aligned} \text{tr}(\mathbf{B} \mathbf{R} \mathbf{B}^H) &= \text{tr}\left(\mathbf{\Theta}^H \mathbf{G}_r^H \mathbf{G}_r \mathbf{\Theta} \mathbf{G}_t \mathbf{R} \mathbf{G}_t^H\right) \\ &= \mathbf{v}^T \left((\mathbf{G}_r^H \mathbf{G}_r) \odot (\mathbf{G}_t \mathbf{R} \mathbf{G}_t^H)^T \right) \mathbf{v}^*. \end{aligned} \quad (44)$$

It is not difficult to check that both $\mathbf{G}_r^H \mathbf{G}_r$ and $\mathbf{G}_t \mathbf{R} \mathbf{G}_t^H$ are positive semidefinite matrices, the Hadamard product of

Algorithm 2 SDR-Based Algorithm for Solving Problem (6)

- 1: **Initialize** IRS phase shifts \mathbf{v} and threshold ε_1 .
- 2: **repeat**
- 3: Update Transmit covariance matrices $\{\mathbf{W}_{c,k}, \mathbf{Z}_r\}$ by solving problem (38).
- 4: Update IRS phase shifts $\{v_m\}$ by solving problem (46).
- 5: **until** the fractional decrease of the objective value of problem (34) is below ε_1 .
- 6: Reconstruct phase shift as $v_m^{\text{opt}} = \frac{v_m}{|v_m|}$, $m \in \mathcal{M}$. Then, using this new reconstructed solution to solve the resulting transmit power minimization problem.
- 7: Construct the rank-one solution of communication beamformers based on (58) and recover radar beamformer based on (59).

$\mathbf{G}_r^H \mathbf{G}_r$ and $(\mathbf{G}_t \mathbf{R} \mathbf{G}_t^H)^T$ is thus a positive semidefinite matrix [62]. This indicates that $\text{tr}(\mathbf{B} \mathbf{R} \mathbf{B}^H)$ in (44) is a quadratic function of \mathbf{v} , which is convex.

As a result, based on (40), (43), and (44), the newly formulated problem is given by

$$\text{Find}\{v_m\} \quad (45a)$$

$$\text{s.t. } f_{1,k}(\mathbf{v}) + \sigma^2 \leq (1/r_{k,\text{th}} + 1) \bar{f}_{2,k}^{\text{lb}}(\mathbf{v}), k \in \mathcal{K}, \quad (45b)$$

$$\begin{aligned} &\text{tr}(\mathbf{A} \mathbf{R} \mathbf{A}^H) \\ &\geq r_{r,\text{th}} \left(\mathbf{v}^T \left((\mathbf{G}_r^H \mathbf{G}_r) \odot (\mathbf{G}_t \mathbf{R} \mathbf{G}_t^H)^T \right) \mathbf{v}^* + \sigma^2 N_r \right), \end{aligned} \quad (45c)$$

$$(37). \quad (45d)$$

It is observed that all constraints are convex, problem (45) is thus convex. However, problem (45) has no explicit objective function. To achieve a better converged solution, we further transform problem (45) into an optimization problem with an explicit objective function to obtain a more efficient IRS phase-shift solution. Specifically, by introducing auxiliary non-negative optimization variables $\{\eta_k, k \in \mathcal{K}\}$ associated with (45b) and η_0 associated with (45c), problem (45) can be recast as

$$\max_{\eta_0 \geq 0, \eta_k \geq 0, \mathbf{v}} \sum_{k=1}^K \eta_k + \eta_0 \quad (46a)$$

$$\text{s.t. } \eta_k + f_{1,k}(\mathbf{v}) + \sigma^2 \leq (1/r_{k,\text{th}} + 1) \bar{f}_{2,k}^{\text{lb}}(\mathbf{v}), k \in \mathcal{K}, \quad (46b)$$

$$\begin{aligned} &\text{tr}(\mathbf{A} \mathbf{R} \mathbf{A}^H) \geq r_{r,\text{th}} \\ &\times \left(\mathbf{v}^T \left((\mathbf{G}_r^H \mathbf{G}_r) \odot (\mathbf{G}_t \mathbf{R} \mathbf{G}_t^H)^T \right) \mathbf{v}^* + \sigma^2 N_r \right) \\ &+ \eta_0, \end{aligned} \quad (46c)$$

$$(37). \quad (46d)$$

It can be checked that problem (46) is convex, which thus can be solved by convex techniques.

C. Overall Algorithm

Based on the above two subproblems, we alternately optimize each subproblem in an iterative way until convergence is

achieved. It is worth pointing out that the converged solution may not satisfy unit-modulus constraint as well as rank-one solution of communication beamformers. As such, additional operations are required. To be specific, we first normalize the amplitudes of IRS phase shifts to be one and solve the resulting Radcom BS transmit power minimization problem based on the new constructed IRS phase shifts. Then, we check whether the rank of $\mathbf{W}_{c,k}, k \in \mathcal{K}$ equals to one or not. If the rank of $\mathbf{W}_{c,k}$ is one, then we can obtain the optimal $\mathbf{w}_{c,k}$ by performing eigenvalue decomposition on $\mathbf{W}_{c,k}$. For the high rank solution (larger than one) of $\mathbf{W}_{c,k}$, the traditional method to extract a rank-one solution from $\mathbf{W}_{c,k}$ is applying the Gaussian randomization technique [63]. However, it inevitably incurs performance loss as well as high computational complexity. Fortunately, the following theorem shows that there always exists the rank-one solution of $\mathbf{W}_{c,k}, k \in \mathcal{K}$ to problem (34).

Theorem 2: There always exists a converged communication beamformer solution, denoted as $\hat{\mathbf{W}}_{c,k}, k \in \mathcal{K}$, satisfying $\text{rank}(\hat{\mathbf{W}}_{c,k}) = 1, k \in \mathcal{K}$.

Proof: Please refer to Appendix C. ■

Theorem 2 shows that the Gaussian randomization technique is not needed in general. We can construct the rank-one solution of communication beamformer based on (58) and recover the radar beamformer based on (59).

The details are summarized in Algorithm 2. The main computational complexity of Algorithm 2 is given by $\mathcal{O}(L_{\text{total}}((K+1)N_t^2)^{3.5} + (M+K+1)^{3.5})$, where L_{total} denotes the total number of iterations required for reaching convergence.

D. Special Case Discussion

It still remains unknown whether the radar signals are really needed in problem (6). Below, we make an in-depth analysis on this question.

Theorem 3: the special case of problem (6) without constraint (6d), the optimal radar beamformer satisfies $\mathbf{w}_{r,i}^{\text{opt}} = \mathbf{0}, i \in \mathcal{N}_t$.

Proof: This result can be directly derived from Theorem 1, and is omitted for brevity. ■

Together with Theorem 1 and Theorem 3, we can conclude that the dedicated radar signals are not needed regardless of the interference provided that the cross-correlation design constraint is not considered.

Theorem 4: For the SDR of problem (6), i.e., problem (34), the optimal radar covariance matrix satisfies $\mathbf{Z}_r^{\text{opt}} = \mathbf{0}$.

Proof: Please refer to Appendix D. ■

Note that although the SDR of problem (6), i.e., problem (34), is equivalent to problem (34)-new defined in Appendix D, the reconstructed rank-one approach proposed in Appendix C is no longer satisfied for problem (34)-new. In general, the SDR tightness for problem (34)-new may not hold due to the limited degrees of freedom of the transmitted signals. As a result, the Gaussian randomization technique may be required to reconstruct the rank-one solution and the performance loss is inevitably incurred [63]. This result indicates that the

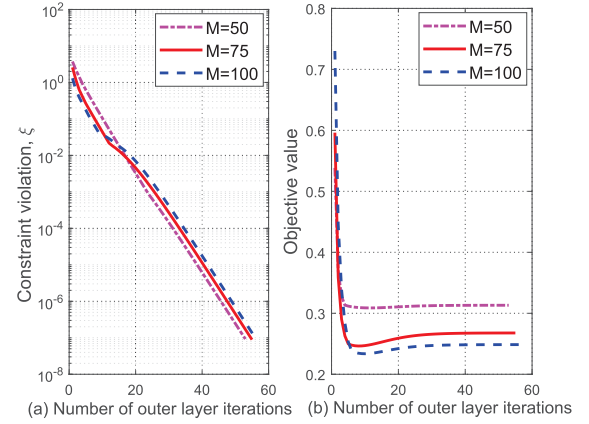


Fig. 2. Convergence behaviour of Algorithm 1.

dedicated radar signals may be required provided that the cross-correlation design constraint is considered.

V. NUMERICAL RESULTS

In this section, we provide numerical results to validate the performance of our proposed joint design of passive and active beamforming in the Radcom system. A three dimensional coordinate setup measured in meter (m) is considered, where the Radcom BS is located at $(0, 0, 3.5)$ m and the users are uniformly and randomly distributed in a circle centered at $(d_x, 0, 1)$ m with a radius 2 m, while the IRS is deployed right above the center of the users at $(d_x, 0, 3.5)$ m, where d_x denotes the horizontal location along x -axis. The distance-dependent path loss model is given by $L(\hat{d}) = c_0(\hat{d}/d_0)^{-\alpha}$, where $c_0 = -30$ dB is the path loss at the reference distance $d_0 = 1$ m, \hat{d} is the link distance, and α is the path loss exponent. We assume that the Radcom BS-IRS link and the IRS-user link follow Rician fading with a Rician factor of 3 dB and a path loss exponent of 2.2, while the BS-user link follows Rayleigh fading with a path loss exponent of 3.6 due to the surrounding rich scatters. Both the transmit and receive antennas at the Radcom are uniform linear arrays with half-wavelength spacing between adjacent antennas, i.e., $d = \lambda/2$. We consider $L = 3$ targets which are located at directions $\theta_1 = -40^\circ$, $\theta_2 = 0^\circ$, and $\theta_3 = 40^\circ$, respectively. In addition, we assume that the communication users have the same SINR constraint, i.e., $r_{c,\text{th}} = r_{k,\text{th}}, k \in \mathcal{K}$. Unless otherwise specified, we set $r_{r,\text{th}} = 10$ dB, $r_{c,\text{th}} = 20$ dB, $N_t = N_r = 8$, $d_x = 50$ m, $\sigma^2 = -80$ dBm, $\sigma_\beta^2 = -70$ dBm, $\rho = 100$, $c = 0.85$, $\varepsilon_1 = 10^{-3}$, and $\varepsilon_2 = 10^{-7}$.

A. Convergence Behavior of the Proposed Two Algorithms

Before discussing the system performance, we first verify the effectiveness of the proposed penalty-based and SDR-based algorithms, i.e., Algorithm 1 and Algorithm 2, respectively.

Fig. 2 shows the constraint violation and convergence of Algorithm 1 by solving problem (7) with $K = 5$ for different number of IRS reflecting elements, namely, $M = 50$, $M = 75$, and $M = 100$. From Fig. 2(a), it is observed that constraint violation ξ decreases fast and reaches the predefined accuracy

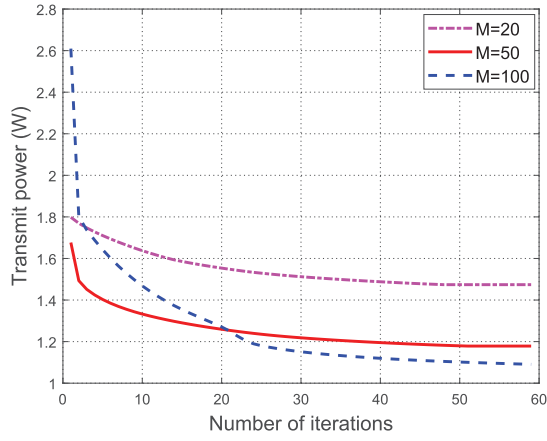


Fig. 3. Convergence behaviour of Algorithm 2.

10^{-7} after about 55 iterations for $M = 50$, which indicates that $\|\mathbf{h}_k^H \mathbf{w}_{c,i} - x_{k,i}^c\|^2$ and $\|\mathbf{A} \mathbf{w}_{c,i} - \mathbf{y}_i^c\|_\infty^2, i \in \mathcal{K}, k \in \mathcal{K}$, in (33) are forced to approach zero. As such, the equality constraint (8d) in problem (8) is eventually satisfied. Even for large M , e.g., $M = 100$, the number of outer layer iterations for reaching the predefined accuracy is about 57 iterations, which again demonstrates the effectiveness of Algorithm 1. In Fig. 2(b), we can observe that the objective value (9a) is not monotonically decreasing with the number of outer layer iterations and fluctuates during the intermediate iterations. This is mainly because when the penalty coefficient ρ is relatively large, the obtained solution does not satisfy the equality in (8d), thus resulting in the oscillatory behavior. However, as ρ becomes very small, the constraint violation is forced to approach the predefined accuracy. Thus, Algorithm 1 is guaranteed to converge finally.

Fig. 3 shows the convergence of Algorithm 2 by solving problem (34) with $K = 5$ and $\epsilon_{th} = \infty$ (i.e., ignore cross-correlation constraint (34d)) for different M . It is observed that the required transmit power is monotonically decreasing with the number of iterations and converges about 58 iterations for different setups. This is expected since each subproblem is optimally/locally solved in each iteration, which results in a non-increasing objective value over iterations. In addition, the objective value is lower-bounded by a finite value due to the minimum SINR required by both users and targets. Thus, Algorithm 2 is guaranteed to converge finally.

B. IRS-Aided Radar and Communication

In this subsection, we compare our proposed scheme with several benchmark schemes under different setups. We adopt the following schemes for comparison:

- **Penalty, no interference scheme:** this corresponds to case I, where both communication signals and radar signals are transmitted and the resulting problem is solved by Algorithm 1.
- **Commun_only, penalty, no interference scheme:** this corresponds to case I, where only communication signals are transmitted and the resulting problem is solved by Algorithm 1.

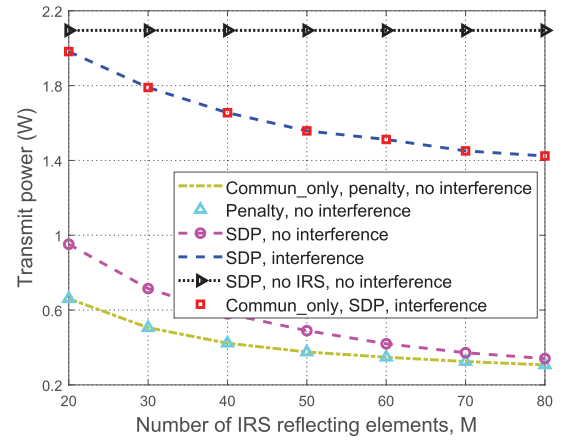


Fig. 4. Transmit power versus the number of IRS elements.

- **SDP, no interference scheme:** this corresponds to case I, where both communication signals and radar signals are transmitted and the resulting problem is solved by Algorithm 2.
- **SDP, no IRS, no interference scheme:** this corresponds to case I, where the IRS is not used and the resulting problem is solved by Algorithm 2.
- **SDP, interference scheme:** this corresponds to case II, where both communication signals and radar signals are transmitted and the resulting problem is solved by Algorithm 2.
- **Commun_only, SDP, interference scheme:** this corresponds to case II, where only communication signals are transmitted and the resulting problem is solved by Algorithm 2.

1) *Effect of Number of IRS Reflecting Elements:* In Fig. 4, we compare the transmit power obtained by all schemes versus M with $K = 5$ and $\epsilon_{th} = \infty$. First, it is observed that with the optimization of IRS phase shifts, the required transmit power monotonically decreases with M , even when the interference exists. This is because that installing more reflecting elements at the IRS is able to provide higher passive beamforming gain towards the desired users, thereby reducing transmit power. Second, it is observed that with the IRS, the schemes without interference significantly outperform those with interference as expected. Third, the “Commun_only, penalty, no interference” scheme achieves the same performance with the “Penalty, no interference” scheme, which implies the radar signals are unnecessary and justifies Theorem 1. In addition, we also observe the same results for the case with interference, which justifies Theorem 3. Last, the penalty-based algorithm achieves lower transmit power than the SDP-based algorithm. This is because that with the proper variables partitioning, there is no constraint coupling between the variables in different blocks as shown in Algorithm 1, while it does not hold in Algorithm 2.

2) *Effect of Number of Users:* In Fig. 5, we compare the transmit power obtained by all schemes versus K with $M = 50$ and $\epsilon_{th} = \infty$. It is observed that the required transmit power obtained by all schemes is monotonically increasing as K increases. This is because that the required transmit power highly depends on the user who has the worst channel

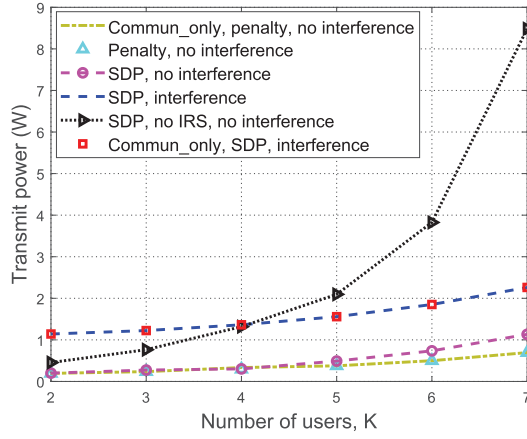


Fig. 5. Transmit power versus the number of users.

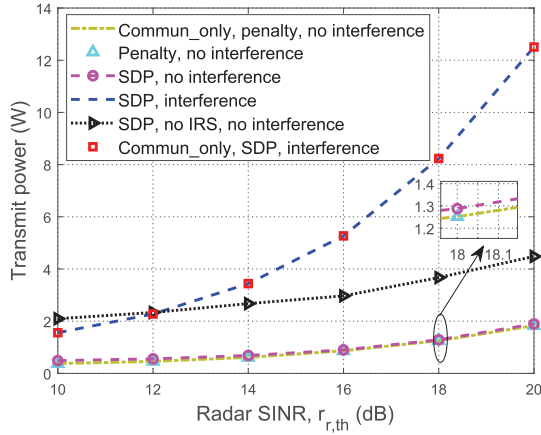


Fig. 6. Transmit power versus the Radar SINR.

quality to satisfy the minimum SINR. In addition, we observe that the scheme without IRS requires much higher transmit power than those with IRS in the without interference case, especially when K becomes large, which demonstrates the benefits of applying IRS in the Radcom system. Furthermore, we observe that the scheme with only communication signal transmission achieves the same transmit power with the joint signal transmission, which again justifies Theorem 1 and Theorem 3.

3) *Effect of Radar SINR*: In Fig. 6, we study the impact of radar SINR $r_{r,th}$ on the transmit power required at the Radcom BS with $K = 5$, $M = 50$, $\epsilon_{th} = \infty$, and $r_{c,th} = 20$ dB. We observe that the required transmit power obtained by the scheme with interference remarkably increases as compared with that obtained by the scheme without interference, especially when the required $r_{r,th}$ is high. This is because that as $r_{r,th}$ becomes large, the interference introduced by the IRS will be more prominent, which thus requires higher transmit power to satisfy the radar SINR. However, if the interference can be perfectly canceled, the scheme with the IRS achieves much lower transmit power than that without IRS due to the high passive beamforming gains brought by the IRS.

4) *Effect of IRS Deployment*: In Fig. 7, we study the impact of IRS deployment/location d_x on the system performance with $M = 50$, $K = 5$, and $\epsilon_{th} = \infty$. We observe that as d_x increases, i.e., the distance between the IRS and the Radcom

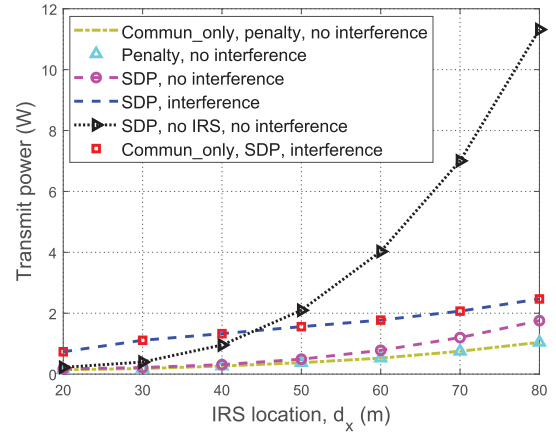
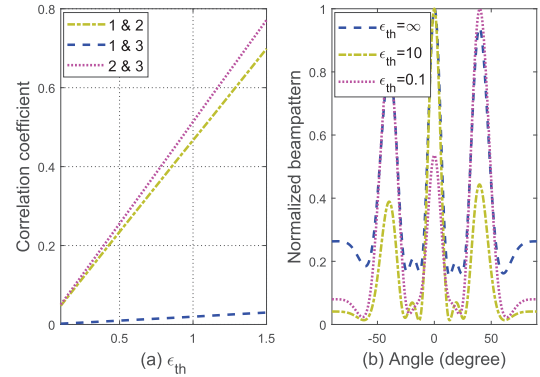
Fig. 7. Transmit power versus IRS location d_x .

Fig. 8. Beampattern design.

BS becomes larger, the required transmit power is remarkably increased by the scheme without IRS due to the high path-loss attenuation. In addition, the performance gap between “SDP, no interference” and “SDP, no IRS, no interference” becomes more pronounced when the IRS is far away from the Radcom BS, which further demonstrates the benefits brought by the IRS. However, this result does not hold for the schemes with interference. To be specific, when $d_x \leq 45$, the “SDP, interference” scheme consumes more transmit power than the “SDP, no IRS, no interference” scheme, while when $d_x \geq 45$, the “SDP, interference” scheme saves more transmit power than the “SDP, no IRS, no interference” scheme. This is because as the IRS is deployed close to the Radcom, i.e., $d_x \leq 45$, the interference introduced by the IRS is significant, thus impairing the system performance. However, as the IRS is far away from the Radcom, i.e., $d_x \geq 45$, the interference introduced by the IRS becomes small. To see it clearly, it is observed that the performance gap between “SDP, interference” and “SDP, no interference” becomes smaller as d_x increases, which indicates that the impact of interference introduced by the IRS on the Radcom becomes smaller.

5) *Effect of Cross-Correlation Constraint*: In Fig. 8(a), we study the impact of ϵ_{th} on the cross-correlation coefficients of the three target reflected signals. It is observed that when ϵ_{th} approaches zero, i.e., $\xi_{th} = 0.1$, which implies that a stringent cross-correlation is imposed, and all cross-correlation coefficients are very small. However, as ϵ_{th} becomes large, the first and second reflected signals, i.e., 1 & 2, and the

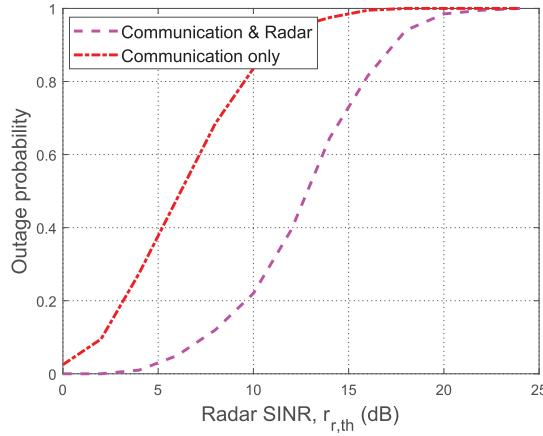


Fig. 9. Outage probability versus Radar SINR.

second and third reflected signals, i.e., 2 & 3, are highly correlated, which can degrade significantly the performance of any adaptive technique for the multi-target radar detection [59]. An example of the normalized magnitudes of beampatterns obtained for different ϵ_{th} under $\beta_l = \sigma_\beta, l \in \mathcal{L}$ is studied in Fig. 8(b). We observe that the beampattern designs obtained by different ϵ_{th} are similar to one another, which has the same observation in [57].

6) *Single Waveform Versus Joint Waveforms*: To evaluate the impact of the single waveform design and the joint waveform design on the system performance. In Fig. 9, we study the outage probability versus Radar SINR $r_{r,th}$ in case II for different transmit beamforming schemes with $K = 5$, $M = 50$, $d_x = 20$, and $\epsilon_{th} = 1$. Two schemes are compared: 1) Communication & Radar: both the communication and radar signals are used for transmission and the resulting problem is solved by Algorithm 2; 2) Communication only: only the communication signal is used for transmission and the resulting problem is solved by Algorithm 2 but the Gaussian randomization technique is applied for reconstructing rank-one solution (Here, 1000 Gaussian randomization realizations are performed). It is observed that the outage probability obtained by the two schemes increases as $r_{r,th}$ increases and finally approaches 1 for large $r_{r,th}$. This is expected since the higher transmit power is required for satisfying the stringent Radar SINR constraint, thereby potentially increasing the cross-correlation coefficient in (34d) and making the problem infeasible with a higher probability. In addition, it is observed that the “Communication & Radar” scheme performs better than the “Communication only” scheme, which indicates that the radar signal is useful for system design.

VI. CONCLUSION

In this paper, we studied the joint design of active beamforming and passive beamforming for an IRS-aided Radcom system. The transmit power minimization problems for two cases, i.e., case I and case II, based on the presence or absence of the radar cross-correlation design and the interference introduced by the IRS on the Radcom BS were formulated. We first studied case I and proved that the dedicated radar signals are not required, and then proposed a penalty-based algorithm

to solve the formulated non-convex optimization problem. Then, we studied case II and showed that the dedicated radar signals are required in general to enhance the system performance, and an SDR-based AO algorithm is proposed to solve this challenging optimization problem. Simulation results demonstrated the benefits of the IRS used for enhancing the performance of the Radcom system. In addition, the results also showed for case II that adopting dedicated radar signals at the Radcom BS can significantly reduce the system outage probability as compared to the case without adopting the dedicated radar signals.

APPENDIX A PROOF OF THEOREM 1

We prove Theorem 1 by solving the SDR of problem (7). Specifically, define $\mathbf{Z}_r = \mathbf{W}_r \mathbf{W}_r^H$ and $\mathbf{W}_{c,k} = \mathbf{w}_{c,k} \mathbf{w}_{c,k}^H, k \in \mathcal{K}$, which need to satisfy $\mathbf{Z}_r \succeq \mathbf{0}, \mathbf{W}_{c,k} \succeq \mathbf{0}$, and $\text{rank}(\mathbf{W}_{c,k}) = 1$. By ignoring the above rank-one constraint on $\mathbf{W}_{c,k}$'s, the SDR of problem (7) for any given IRS phase shifts \mathbf{v} is given by

$$\min_{\{\mathbf{W}_{c,k}\}, \mathbf{Z}_r} \sum_{k=1}^K \text{tr}(\mathbf{W}_{c,k}) + \text{tr}(\mathbf{Z}_r) \quad (47a)$$

$$\text{s.t. } \mathbf{h}_k^H \left(\sum_{k=1}^K \mathbf{W}_{c,k} + \mathbf{Z}_r \right) \mathbf{h}_k + \sigma^2 \leq \left(\frac{1}{r_{k,th}} + 1 \right) \mathbf{h}_k^H \mathbf{W}_{c,k} \mathbf{h}_k, k \in \mathcal{K}, \quad (47b)$$

$$\text{tr} \left(\mathbf{A} \left(\sum_{k=1}^K \mathbf{W}_{c,k} + \mathbf{Z}_r \right) \mathbf{A}^H \right) \geq r_{r,th} \sigma^2. \quad (47c)$$

It is not difficult to see that problem (47) is a semidefinite programming (SDP) problem and satisfies the Slater's condition, which indicates that the duality gap is zero. Thus, we consider the following Lagrangian of problem (47) given by

$$\begin{aligned} \mathcal{L}_1 \{ \{\mathbf{W}_{c,k}\}, \mathbf{Z}_r, \{\lambda_{1,k}\}, \mu \} \\ = \sum_{k=1}^K \text{tr}(\mathbf{B}_k \mathbf{W}_{c,k}) \\ + \text{tr}(\mathbf{C} \mathbf{Z}_r) + \sum_{k=1}^K \lambda_{1,k} \sigma^2 + \mu \sigma^2 r_{r,th}, \end{aligned} \quad (48)$$

where

$$\begin{aligned} \mathbf{B}_k = \mathbf{I}_{N_t} + \sum_{i \neq k}^K \lambda_{1,i} \mathbf{h}_i \mathbf{h}_i^H \\ - \lambda_{1,k} \mathbf{h}_k \mathbf{h}_k^H / r_{k,th} - \mu \mathbf{A}^H \mathbf{A}, \quad k \in \mathcal{K}, \end{aligned} \quad (49)$$

$$\mathbf{C} = \mathbf{I}_{N_t} + \sum_{k=1}^K \lambda_{1,k} \mathbf{h}_k \mathbf{h}_k^H - \mu \mathbf{A}^H \mathbf{A}, \quad (50)$$

and $\{\lambda_{1,k} \geq 0\}$ and $\mu \geq 0$ are the dual variables associated with constraints (47b) and (47c), respectively. Denote by dual function $f_1 \{ \{\lambda_{1,k}\}, \mu \} = \min_{\{\mathbf{W}_{c,k}\}, \mathbf{Z}_r} \mathcal{L}_1 \{ \{\mathbf{W}_{c,k}\}, \mathbf{Z}_r, \{\lambda_{1,k}\}, \mu \}$, we have the following lemma:

Lemma 1: To make dual function $f_1 \{\{\lambda_{1,k}\}, \mu\}$ bounded, we must have

$$\mathbf{C} \succeq \mathbf{0}, \quad \mathbf{B}_k \succeq \mathbf{0}, \quad k \in \mathcal{K}. \quad (51)$$

Proof: This can be proved by contradiction. Suppose that \mathbf{B}_k (\mathbf{C}) has at least one negative eigenvalue, we can always construct a solution of $\mathbf{W}_{c,k}(\mathbf{Z}_r)$ that has the same eigenvectors with \mathbf{B}_k (\mathbf{C}), while the eigenvalues of $\mathbf{W}_{c,k}(\mathbf{Z}_r)$ corresponding to \mathbf{B}_k (\mathbf{C}) with negative eigenvalues are set to be positive infinity, resulting in $\text{tr}(\mathbf{B}_k \mathbf{W}_{c,k}) \rightarrow -\infty$ and $\text{tr}(\mathbf{C} \mathbf{Z}_r) \rightarrow -\infty$. This thus completes the proof. ■

Accordingly, the dual problem of (47) is given by

$$\max_{\{\lambda_{1,k} \geq 0\}, \mu \geq 0} \sum_{k=1}^K \lambda_{1,k} \sigma^2 + \mu \sigma_r^2 r_{r,\text{th}} \quad (52a)$$

$$\text{s.t. } \mathbf{C} \succeq \mathbf{0}, \quad \mathbf{B}_k \succeq \mathbf{0}, \quad k \in \mathcal{K}. \quad (52b)$$

Based on Lemma 1, it is not difficult to prove that at optimal solutions $\{\mathbf{W}_{c,k}^{\text{opt}}, \mathbf{Z}_r^{\text{opt}}\}$ to minimize (48) for fixed dual variables, the following equalities must hold:

$$\text{tr}(\mathbf{C}^{\text{opt}} \mathbf{Z}_r^{\text{opt}}) = 0, \quad \text{tr}(\mathbf{B}_k^{\text{opt}} \mathbf{W}_{c,k}^{\text{opt}}) = 0, \quad k \in \mathcal{K}, \quad (53)$$

which are equivalent to $\mathbf{C}^{\text{opt}} \mathbf{Z}_r^{\text{opt}} = \mathbf{0}$ and $\mathbf{B}_k^{\text{opt}} \mathbf{W}_{c,k}^{\text{opt}} = \mathbf{0}, k \in \mathcal{K}$.

To prove Theorem 1, we need to prove that the optimal solutions of problem (47) should satisfy $\text{rank}(\mathbf{W}_{c,k}^{\text{opt}}) = 1, k \in \mathcal{K}$, and $\mathbf{Z}_r^{\text{opt}} = \mathbf{0}$. To proceed it, we consider the following two cases: 1) $\lambda_{1,k}^{\text{opt}} = 0$ for $k \in \mathcal{K}$; 2) at least one $\lambda_{1,k}^{\text{opt}}$ for $k \in \mathcal{K}$ is not equal to zero.

For the first case, it is not difficult to see that $\mathbf{C}^{\text{opt}} = \mathbf{B}_k^{\text{opt}} = \mathbf{I}_{N_t} - \mu^{\text{opt}} \mathbf{A}^H \mathbf{A}, k \in \mathcal{K}$. To guarantee $\mathbf{B}_k^{\text{opt}} \succeq \mathbf{0}, k \in \mathcal{K}$, and maximize dual problem (52), the optimal dual variable μ^{opt} should satisfy $\mu^{\text{opt}} = 1/\pi_{\max}$, where π_{\max} represents the maximum eigenvalue of $\mathbf{A}^H \mathbf{A}$. Under the assumption that amplitudes of targets are independently distributed, i.e., the non-zero singular values of $\mathbf{A}^H \mathbf{A}$ are not the same, \mathbf{C}^{opt} and $\mathbf{B}_k^{\text{opt}}$ must have only one zero eigenvalue and satisfy $\text{rank}(\mathbf{C}^{\text{opt}}) = \text{rank}(\mathbf{B}_k^{\text{opt}}) = N_t - 1, k \in \mathcal{K}$. Denote by \mathbf{v}_{\max} the eigenvector corresponding to the maximum eigenvalue of $\mathbf{A}^H \mathbf{A}$. It is readily to see that $\mathbf{Z}_r^{\text{opt}}$ and $\mathbf{W}_{c,k}^{\text{opt}}$ should all lie in the subspace spanned by \mathbf{v}_{\max} . This indicates that all communication beams should point towards the targets rather than the communication users and the minimum user SINR requirements in (47b) will not be satisfied any more. Obviously, the case of $\lambda_{1,k}^{\text{opt}} = 0, k \in \mathcal{K}$, cannot occur here.

For the second case, with any given $\mathbf{Z}_r^{\text{opt}} \succeq \mathbf{0}$ satisfying (53), we have

$$\begin{aligned} & -(1/r_{k,\text{th}} + 1) \lambda_{1,k}^{\text{opt}} \mathbf{h}_k^H \mathbf{Z}_r^{\text{opt}} \mathbf{h}_k \\ &= \text{tr}(\mathbf{C}^{\text{opt}} \mathbf{Z}_r^{\text{opt}} - (1/r_{k,\text{th}} + 1) \lambda_{1,k} \mathbf{h}_k \mathbf{h}_k^H \mathbf{Z}_r^{\text{opt}}) \\ &= \text{tr}(\mathbf{B}_k^{\text{opt}} \mathbf{Z}_r^{\text{opt}}) \geq 0, \end{aligned} \quad (54)$$

where the first equality follows from (53), the second equality follows from (49) and (50), and the last inequality holds since both $\mathbf{B}_k^{\text{opt}}$ and $\mathbf{Z}_r^{\text{opt}}$ are positive semidefinite matrices. From (54), we can derive $\lambda_{1,k}^{\text{opt}} \text{tr}(\mathbf{h}_k \mathbf{h}_k^H \mathbf{Z}_r^{\text{opt}}) = 0$

since $\lambda_{1,k}^{\text{opt}} \geq 0$ and $\mathbf{h}_k^H \mathbf{Z}_r^{\text{opt}} \mathbf{h}_k \geq 0, k \in \mathcal{K}$. As a result, based on (53) and together with $\lambda_{1,k}^{\text{opt}} \text{tr}(\mathbf{h}_k \mathbf{h}_k^H \mathbf{Z}_r^{\text{opt}}) = 0$, we have

$$\begin{aligned} & (\mathbf{I}_{N_t} - \mu^{\text{opt}} \mathbf{A}^H \mathbf{A}) \mathbf{Z}_r^{\text{opt}} \\ &= \left(\mathbf{I}_{N_t} + \sum_{k=1}^K \lambda_{1,k}^{\text{opt}} \mathbf{h}_k \mathbf{h}_k^H - \mu \mathbf{A}^H \mathbf{A} \right) \mathbf{Z}_r^{\text{opt}} = \mathbf{0}. \end{aligned} \quad (55)$$

Suppose that $\lambda_{1,m}^{\text{opt}}$ is the non-zero eigenvalue, i.e., $\lambda_{1,m}^{\text{opt}} > 0$, it follows that $\mathbf{h}_m \mathbf{h}_m^H \mathbf{Z}_r^{\text{opt}} = \mathbf{0}$. Since the non-zero singular values of $\mathbf{A}^H \mathbf{A}$ are not the same, we have $\text{rank}(\mathbf{I}_{N_t} - \mu^{\text{opt}} \mathbf{A}^H \mathbf{A}) \geq N_t - 1$. This indicates that two matrices $\mathbf{I}_{N_t} - \mu^{\text{opt}} \mathbf{A}^H \mathbf{A}$ and $\mathbf{h}_m \mathbf{h}_m^H$ span the entire space with probability one under the assumption that amplitudes of targets and user channels are uncorrelated. As such, we must have $\mathbf{Z}_r^{\text{opt}} = \mathbf{0}$.

Next, we show to prove $\text{rank}(\mathbf{W}_{c,k}^{\text{opt}}) = 1, k \in \mathcal{K}$. On the one hand, based on (53), it follows that $\text{rank}(\mathbf{B}_k^{\text{opt}}) \leq N_t - 1$ since $\mathbf{W}_{c,k}^{\text{opt}} \neq \mathbf{0}$ (otherwise the communication user SINR constraint (47b) will not be satisfied). On the other hand, recall that any $\mathbf{Z}_r^{\text{opt}} \succeq \mathbf{0}$ satisfying (53) should be 0, it follows that $\text{rank}(\mathbf{C}^{\text{opt}}) = N_t$. Based on (49) and (50), we have

$$\begin{aligned} \text{rank}(\mathbf{B}_k^{\text{opt}}) &= \text{rank}(\mathbf{C}^{\text{opt}} - (1/r_{k,\text{th}} + 1) \lambda_{1,k}^{\text{opt}} \mathbf{h}_k \mathbf{h}_k^H) \\ &\geq \text{rank}(\mathbf{C}^{\text{opt}}) - \text{rank}((1/r_{k,\text{th}} + 1) \lambda_{1,k}^{\text{opt}} \mathbf{h}_k \mathbf{h}_k^H) \\ &= N_t - 1. \end{aligned} \quad (56)$$

Thus, combining arguments $\mathbf{B}_k^{\text{opt}} \leq N_t - 1$ and $\mathbf{B}_k^{\text{opt}} \geq N_t - 1$, we have $\mathbf{B}_k^{\text{opt}} = N_t - 1, k \in \mathcal{K}$. Based on (53), it follows $\text{rank}(\mathbf{W}_{c,k}^{\text{opt}}) = 1, k \in \mathcal{K}$. Together with the facts that $\mathbf{Z}_r^{\text{opt}} = \mathbf{0}$ and $\text{rank}(\mathbf{W}_{c,k}^{\text{opt}}) = 1, k \in \mathcal{K}$, we can conclude that problem (47) is equivalent to problem (7) and no radar beams are required, which completes the proof.

APPENDIX B PROOF OF LEMMA 2

To show Lemma 2, we expand Lagrangian function (19) as

$$\begin{aligned} & \mathcal{L}_2(x_{k,i}^c, \lambda_{2,k}) \\ &= (1 - \lambda_{2,k}) |x_{k,k}^c|^2 - 2\text{Re}\{x_{k,k}^{c,H} \mathbf{h}_k^H \mathbf{w}_{c,k}\} \\ & \quad + |\mathbf{h}_k^H \mathbf{w}_{c,k}|^2 + \sum_{i \neq k}^K (|\mathbf{h}_k^H \mathbf{w}_{c,i} - x_{k,i}^c|^2 + \lambda_{2,k} r_{k,\text{th}} |x_{k,i}^c|^2) \\ & \quad + \lambda_{2,k} r_{k,\text{th}} \sigma^2. \end{aligned} \quad (57)$$

To make dual function $f_2(\lambda_{2,k}) = \min_{x_{k,i}^c} \mathcal{L}_2(x_{k,i}^c, \lambda_{2,k})$ bounded, we should make $1 - \lambda_{2,k} > 0$, i.e., $\lambda_{2,k} < 1$, since otherwise we can always set $x_{k,k}^c = \kappa \mathbf{h}_k^H \mathbf{w}_{c,k}$ and let κ to be positive infinity, which will make $f_2(\lambda_{2,k})$ unbounded. This thus completes the proof of Lemma 2.

APPENDIX C PROOF OF THEOREM 2

Suppose that $\{\bar{\mathbf{W}}_{c,k}, \bar{\mathbf{Z}}_r\}$ are the converged solutions obtained by AO approach to problem (34). We then construct

another new solutions $\{\hat{\mathbf{W}}_{c,k}, \hat{\mathbf{Z}}_r\}$ that satisfy

$$\begin{aligned}\hat{\mathbf{w}}_{c,k} &= (\mathbf{h}_k^H \bar{\mathbf{W}}_{c,k} \mathbf{h}_k)^{-1/2} \bar{\mathbf{W}}_{c,k} \mathbf{h}_k, \\ \hat{\mathbf{W}}_{c,k} &= \hat{\mathbf{w}}_{c,k} \hat{\mathbf{w}}_{c,k}^H, \quad k \in \mathcal{K},\end{aligned}\quad (58)$$

$$\hat{\mathbf{Z}}_r = \sum_{k=1}^K \bar{\mathbf{W}}_{c,k} + \bar{\mathbf{Z}}_r - \sum_{k=1}^K \hat{\mathbf{W}}_{c,k}, \quad k \in \mathcal{K}. \quad (59)$$

To prove Theorem 2, we need to prove: 1) $\text{rank}(\hat{\mathbf{W}}_{c,k}) = 1, \hat{\mathbf{W}}_{c,k} \succeq \mathbf{0}, \hat{\mathbf{Z}}_r \succeq \mathbf{0}$; 2) the objective value obtained by $\{\hat{\mathbf{W}}_{c,k}, \hat{\mathbf{Z}}_r\}$ in (34a) remains unchanged; 3) all constraints (34b)-(34d) are still satisfied.

First, based on (58), it is not difficult to check that the newly constructed solutions $\hat{\mathbf{W}}_{c,k}, k \in \mathcal{K}$ are rank-one and positive semidefinite, i.e., satisfy $\text{rank}(\hat{\mathbf{W}}_{c,k}) = 1, \hat{\mathbf{W}}_{c,k} \succeq \mathbf{0}$. In addition, for any $\phi \in \mathbb{C}^{N_t \times 1} \neq \mathbf{0}$, we have

$$\begin{aligned}\phi^H (\bar{\mathbf{W}}_{c,k} - \hat{\mathbf{W}}_{c,k}) \phi \\ = \phi^H \bar{\mathbf{W}}_{c,k} \phi - (\mathbf{h}_k^H \bar{\mathbf{W}}_{c,k} \mathbf{h}_k)^{-1} |\phi^H \bar{\mathbf{W}}_{c,k} \mathbf{h}_k|^2 \geq 0,\end{aligned}\quad (60)$$

where the last inequality follows from identity $|\phi^H \bar{\mathbf{W}}_{c,k} \mathbf{h}_k|^2 \leq (\phi^H \bar{\mathbf{W}}_{c,k} \phi) (\mathbf{h}_k^H \bar{\mathbf{W}}_{c,k} \mathbf{h}_k)$ according to the Cauchy-Schwarz inequality. From (60), it indicates that $\bar{\mathbf{W}}_{c,k} - \hat{\mathbf{W}}_{c,k} \succeq \mathbf{0}$. Thus, we can see from (59) that $\hat{\mathbf{Z}}_r$ can be rewrote as the summation of $K+1$ positive semidefinite matrices, it follows that $\hat{\mathbf{Z}}_r \succeq \mathbf{0}$.

Second, the expression $\sum_{k=1}^K \hat{\mathbf{W}}_{c,k} + \hat{\mathbf{Z}}_r$ can be recast as

$$\begin{aligned}\sum_{k=1}^K \hat{\mathbf{W}}_{c,k} + \hat{\mathbf{Z}}_r &= \sum_{k=1}^K \hat{\mathbf{W}}_{c,k} + \sum_{k=1}^K \bar{\mathbf{W}}_{c,k} + \bar{\mathbf{Z}}_r - \sum_{k=1}^K \hat{\mathbf{W}}_{c,k} \\ &= \sum_{k=1}^K \bar{\mathbf{W}}_{c,k} + \bar{\mathbf{Z}}_r,\end{aligned}\quad (61)$$

where the first equality follows from (59). Thus, we have $\sum_{k=1}^K \text{tr}(\hat{\mathbf{W}}_{c,k}) + \text{tr}(\hat{\mathbf{Z}}_r) = \sum_{k=1}^K \text{tr}(\bar{\mathbf{W}}_{c,k}) + \text{tr}(\bar{\mathbf{Z}}_r)$, which shows that the objective value remains unchanged.

Third, substituting (58) into $\mathbf{h}_k^H \hat{\mathbf{W}}_{c,k} \mathbf{h}_k$, we have

$$\mathbf{h}_k^H \hat{\mathbf{W}}_{c,k} \mathbf{h}_k = \mathbf{h}_k^H \hat{\mathbf{w}}_{c,k} \hat{\mathbf{w}}_{c,k}^H \mathbf{h}_k = \mathbf{h}_k^H \bar{\mathbf{W}}_{c,k} \mathbf{h}_k, \quad k \in \mathcal{K}. \quad (62)$$

Combining (62) with (61), we can readily check that constraints (34b)-(34d) are all satisfied. Based on the above results, we complete the proof of Theorem 2.

APPENDIX D PROOF OF THEOREM 4

By setting $\mathbf{Z}_r = \mathbf{0}$ in problem (34) and denoting the newly formulated problem as problem (34)-new, it is not difficult to see that any feasible solutions to problem (34)-new are also feasible to problem (34). Denoted by $\{\tilde{\mathbf{W}}_{c,k}, \tilde{\mathbf{Z}}_r\}$ the feasible

solutions to problem (34). We can always construct another solutions to problem (34)-new, denoted by $\{\hat{\mathbf{W}}_{c,k}\}$, satisfying

$$\hat{\mathbf{W}}_{c,k} = \tilde{\mathbf{W}}_{c,k} + \alpha_k \tilde{\mathbf{Z}}_r, \quad \sum_{k=1}^K \alpha_k = 1, \alpha_k \geq 0, \quad \forall k, \quad (63)$$

so that $\sum_{k=1}^K \hat{\mathbf{W}}_{c,k} = \sum_{k=1}^K \tilde{\mathbf{W}}_{c,k} + \tilde{\mathbf{Z}}_r$ and $\alpha_k \mathbf{h}_k^H \tilde{\mathbf{Z}}_r \mathbf{h}_k \geq 0$, which indicates that any feasible solutions to problem (34) are also feasible to problem (34)-new while with the same objective value. Thus, problem (34) is equivalent to problem (34)-new. This thus completes the proof.

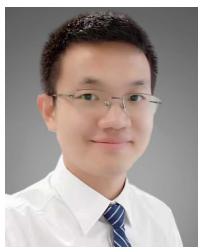
REFERENCES

- [1] T. S. Rappaport *et al.*, "Millimeter wave mobile communications for 5G cellular: It will work!" *IEEE Access*, vol. 1, pp. 335–349, 2013.
- [2] M. Parker, *Digital Signal Processing 101: Everything You Need to Know to Get Started*. London, U.K.: Newnes, 2017.
- [3] L. Zheng, M. Lops, Y. C. Eldar, and X. Wang, "Radar and communication coexistence: An overview: A review of recent methods," *IEEE Signal Process. Mag.*, vol. 36, no. 5, pp. 85–99, Sep. 2019.
- [4] R. Saruthirathanaworakun, J. M. Peha, and L. M. Correia, "Opportunistic sharing between rotating radar and cellular," *IEEE J. Sel. Areas Commun.*, vol. 30, no. 10, pp. 1900–1910, Nov. 2012.
- [5] F. Liu, C. Masouros, A. Li, H. Sun, and L. Hanzo, "MU-MIMO communications with MIMO radar: From co-existence to joint transmission," *IEEE Trans. Wireless Commun.*, vol. 17, no. 4, pp. 2755–2770, Apr. 2018.
- [6] S. Sodagari, A. Khawar, T. C. Clancy, and R. McGwier, "A projection based approach for radar and telecommunication systems coexistence," in *Proc. IEEE Global Commun. Conf. (GLOBECOM)*, Anaheim, CA, USA, Dec. 2012, pp. 5010–5014.
- [7] B. Li, A. P. Petropulu, and W. Trappe, "Optimum co-design for spectrum sharing between matrix completion based MIMO radars and a MIMO communication system," *IEEE Trans. Signal Process.*, vol. 64, no. 17, pp. 4562–4575, Sep. 2016.
- [8] B. Li and A. Petropulu, "MIMO radar and communication spectrum sharing with clutter mitigation," in *Proc. IEEE Radar Conf. (RadarConf)*, Philadelphia, PA, USA, May 2016, pp. 1–6.
- [9] A. Hassanien, M. G. Amin, Y. D. Zhang, and F. Ahmad, "Signaling strategies for dual-function radar communications: An overview," *IEEE Aerosp. Electron. Syst. Mag.*, vol. 31, no. 10, pp. 36–45, Oct. 2016.
- [10] A. Liu *et al.*, "A survey on fundamental limits of integrated sensing and communication," *IEEE Commun. Surveys Tuts.*, vol. 24, no. 2, pp. 994–1034, 2nd Quart., 2022.
- [11] J. A. Zhang *et al.*, "An overview of signal processing techniques for joint communication and radar sensing," *IEEE J. Sel. Topics Signal Process.*, vol. 15, no. 6, pp. 1295–1315, Nov. 2021.
- [12] C. Sturm and W. Wiesbeck, "Waveform design and signal processing aspects for fusion of wireless communications and radar sensing," *Proc. IEEE*, vol. 99, no. 7, pp. 1236–1259, Jul. 2011.
- [13] A. Hassanien, M. G. Amin, Y. D. Zhang, and F. Ahmad, "Dual-function radar-communications: Information embedding using sidelobe control and waveform diversity," *IEEE Trans. Signal Process.*, vol. 64, no. 8, pp. 2168–2181, Apr. 2016.
- [14] A. Hassanien, M. G. Amin, Y. D. Zhang, and F. Ahmad, "Phase-modulation based dual-function radar-communications," *IET Radar, Sonar Navigat.*, vol. 10, no. 8, pp. 1411–1421, 2016.
- [15] A. Şahin, S. S. M. Hoque, and C.-Y. Chen, "Index modulation with circularly-shifted chirps for dual-function radar and communications," *IEEE Trans. Wireless Commun.*, vol. 21, no. 5, pp. 2938–2952, May 2022.
- [16] F. Liu, L. Zhou, C. Masouros, A. Li, W. Luo, and A. Petropulu, "Toward dual-functional radar-communication systems: Optimal waveform design," *IEEE Trans. Signal Process.*, vol. 66, no. 16, pp. 4264–4279, Aug. 2018.

- [17] R. Liu, M. Li, Q. Liu, and A. L. Swindlehurst, "Dual-functional radar-communication waveform design: A symbol-level precoding approach," *IEEE J. Sel. Topics Signal Process.*, vol. 15, no. 6, pp. 1316–1331, Nov. 2021.
- [18] X. Liu, T. Huang, N. Shlezinger, Y. Liu, J. Zhou, and Y. C. Eldar, "Joint transmit beamforming for multiuser MIMO communications and MIMO radar," *IEEE Trans. Signal Process.*, vol. 68, pp. 3929–3944, 2020.
- [19] H. Hua, J. Xu, and T. Xiao Han, "Optimal transmit beamforming for integrated sensing and communication," 2021, *arXiv:2104.11871*.
- [20] Q. Wu and R. Zhang, "Towards smart and reconfigurable environment: Intelligent reflecting surface aided wireless network," *IEEE Commun. Mag.*, vol. 58, no. 1, pp. 106–112, Jan. 2020.
- [21] Q. Wu, S. Zhang, B. Zheng, C. You, and R. Zhang, "Intelligent reflecting surface aided wireless communications: A tutorial," 2020, *arXiv:2007.02759*.
- [22] Y. Liu *et al.*, "Reconfigurable intelligent surfaces: Principles and opportunities," *IEEE Commun. Surveys Tuts.*, vol. 23, no. 3, pp. 1546–1577, 3rd Quart., 2021.
- [23] S. Zhang *et al.*, "Intelligent omni-surfaces: Ubiquitous wireless transmission by reflective-refractive metasurfaces," *IEEE Trans. Wireless Commun.*, vol. 21, no. 1, pp. 219–233, Jan. 2022.
- [24] J. Xu *et al.*, "Simultaneously transmitting and reflecting intelligent omni-surfaces: Modeling and implementation," *IEEE Veh. Technol. Mag.*, vol. 17, no. 2, pp. 46–54, Jun. 2022.
- [25] Y. Liu *et al.*, "STAR: Simultaneous transmission and reflection for 360° coverage by intelligent surfaces," *IEEE Wireless Commun.*, vol. 28, no. 6, pp. 102–109, Dec. 2021.
- [26] Q. Wu and R. Zhang, "Intelligent reflecting surface enhanced wireless network via joint active and passive beamforming," *IEEE Trans. Wireless Commun.*, vol. 18, no. 11, pp. 5394–5409, Nov. 2019.
- [27] Q. Q. Wu and R. Zhang, "Beamforming optimization for wireless network aided by intelligent reflecting surface with discrete phase shifts," *IEEE Trans. Commun.*, vol. 68, no. 3, pp. 1838–1851, May 2020.
- [28] C. Pan *et al.*, "Multicell MIMO communications relying on intelligent reflecting surfaces," *IEEE Trans. Wireless Commun.*, vol. 19, no. 8, pp. 5218–5233, May 2020.
- [29] M. Hua, Q. Wu, D. W. K. Ng, J. Zhao, and L. Yang, "Intelligent reflecting surface-aided joint processing coordinated multipoint transmission," *IEEE Trans. Commun.*, vol. 69, no. 3, pp. 1650–1665, Mar. 2021.
- [30] G. Zhou, C. Pan, H. Ren, K. Wang, and A. Nallanathan, "Intelligent reflecting surface aided multigroup multicast miso communication systems," *IEEE Trans. Signal Process.*, vol. 68, pp. 3236–3251, 2020.
- [31] D. Zhao, H. Lu, Y. Wang, H. Sun, and Y. Gui, "Joint power allocation and user association optimization for IRS-assisted mmWave systems," *IEEE Trans. Wireless Commun.*, vol. 21, no. 1, pp. 577–590, Jan. 2022.
- [32] H. Guo, Y.-C. Liang, J. Chen, and E. G. Larsson, "Weighted sum-rate maximization for intelligent reflecting surface enhanced wireless networks," in *Proc. IEEE Global Commun. Conf. (GLOBECOM)*, Waikoloa, HI, USA, Dec. 2019, pp. 1–6.
- [33] Q. Wu, X. Zhou, and R. Schober, "IRS-assisted wireless powered NOMA: Do we really need different phase shifts in DL and UL?" *IEEE Wireless Commun. Lett.*, vol. 10, no. 7, pp. 1493–1497, Jul. 2021.
- [34] M. Hua and Q. Wu, "Joint dynamic passive beamforming and resource allocation for IRS-aided full-duplex WPCN," *IEEE Trans. Wireless Commun.*, vol. 21, no. 7, pp. 4829–4843, Jul. 2022.
- [35] G. Chen, Q. Wu, W. Chen, D. W. K. Ng, and L. Hanzo, "IRS-aided wireless powered MEC systems: TDMA or NOMA for computation offloading?" *IEEE Trans. Wireless Commun.*, early access, Sep. 12, 2021, doi: [10.1109/TWC.2022.3203158](https://doi.org/10.1109/TWC.2022.3203158).
- [36] H. Long *et al.*, "Reflections in the sky: Joint trajectory and passive beamforming design for secure UAV networks with reconfigurable intelligent surface," 2020, *arXiv:2005.10559*.
- [37] M. Hua, L. Yang, Q. Wu, C. Pan, C. Li, and A. Lee Swindlehurst, "UAV-assisted intelligent reflecting surface symbiotic radio system," *IEEE Trans. Wireless Commun.*, vol. 20, no. 9, pp. 5769–5785, Sep. 2021.
- [38] S. Li, B. Duo, M. D. Renzo, M. Tao, and X. Yuan, "Robust secure UAV communications with the aid of reconfigurable intelligent surfaces," *IEEE Trans. Wireless Commun.*, vol. 20, no. 10, pp. 6402–6417, Apr. 2021.
- [39] K. Meng, Q. Wu, S. Ma, W. Chen, and T. Q. S. Quek, "UAV trajectory and beamforming optimization for integrated periodic sensing and communication," *IEEE Wireless Commun. Lett.*, vol. 11, no. 6, pp. 1211–1215, Jun. 2022.
- [40] X. Mu, Y. Liu, L. Guo, J. Lin, and N. Al-Dhahir, "Exploiting intelligent reflecting surfaces in NOMA networks: Joint beamforming optimization," *IEEE Trans. Wireless Commun.*, vol. 19, no. 10, pp. 6884–6898, Oct. 2020.
- [41] X. Mu, Y. Liu, L. Guo, J. Lin, and N. Al-Dhahir, "Capacity and optimal resource allocation for IRS-assisted multi-user communication systems," *IEEE Trans. Commun.*, vol. 69, no. 6, pp. 3771–3786, Jun. 2021.
- [42] M. Fu, Y. Zhou, Y. Shi, and K. B. Letaief, "Reconfigurable intelligent surface empowered downlink non-orthogonal multiple access," *IEEE Trans. Commun.*, vol. 69, no. 6, pp. 3802–3817, Jun. 2021.
- [43] S. Buzzi, E. Grossi, M. Lops, and L. Venturino, "Foundations of MIMO radar detection aided by reconfigurable intelligent surfaces," *IEEE Trans. Signal Process.*, vol. 70, pp. 1749–1763, 2022.
- [44] W. Lu *et al.*, "Target detection in intelligent reflecting surface aided distributed MIMO radar systems," *IEEE Sensors Lett.*, vol. 5, no. 3, Mar. 2021, Art. no. 7000804.
- [45] C. J. Vaca-Rubio, P. Ramirez-Espinosa, K. Kansanen, Z.-H. Tan, and E. de Carvalho, "Radio sensing with large intelligent surface for 6G," 2021, *arXiv:2111.02783*.
- [46] S. Buzzi, E. Grossi, M. Lops, and L. Venturino, "Radar target detection aided by reconfigurable intelligent surfaces," *IEEE Signal Process. Lett.*, vol. 28, pp. 1315–1319, 2021.
- [47] X. Shao, C. You, W. Ma, X. Chen, and R. Zhang, "Target sensing with intelligent reflecting surface: Architecture and performance," *IEEE J. Sel. Areas Commun.*, vol. 40, no. 7, pp. 2070–2084, Jul. 2022.
- [48] Z.-M. Jiang *et al.*, "Intelligent reflecting surface aided dual-function radar and communication system," *IEEE Syst. J.*, vol. 16, no. 1, pp. 475–486, Mar. 2022.
- [49] X. Song, D. Zhao, H. Hua, T. X. Han, X. Yang, and J. Xu, "Joint transmit and reflective beamforming for IRS-assisted integrated sensing and communication," in *Proc. IEEE Wireless Commun. Netw. Conf. (WCNC)*, Apr. 2022, pp. 189–194.
- [50] X. Wang, Z. Fei, Z. Zheng, and J. Guo, "Joint waveform design and passive beamforming for RIS-assisted dual-functional radar-communication system," *IEEE Trans. Veh. Technol.*, vol. 70, no. 5, pp. 5131–5136, May 2021.
- [51] R. Liu, M. Li, Y. Liu, Q. Wu, and Q. Liu, "Joint transmit waveform and passive beamforming design for RIS-aided DFRC systems," *IEEE J. Sel. Topics Signal Process.*, vol. 16, no. 5, pp. 995–1010, Aug. 2022.
- [52] Y. Wang, H. Lu, and H. Sun, "Channel estimation in IRS-enhanced mmWave system with super-resolution network," *IEEE Commun. Lett.*, vol. 25, no. 8, pp. 2599–2603, Aug. 2021.
- [53] E. Fishler, A. Haimovich, R. S. Blum, L. J. Cimini, D. Chizhik, and R. A. Valenzuela, "Spatial diversity in radars-models and detection performance," *IEEE Trans. Signal Process.*, vol. 54, no. 3, pp. 823–838, Mar. 2006.
- [54] G. Cui, H. Li, and M. Rangaswamy, "MIMO radar waveform design with constant modulus and similarity constraints," *IEEE Trans. Signal Process.*, vol. 62, no. 2, pp. 343–353, Jan. 2014.
- [55] Z. Cheng, Z. He, B. Liao, and M. Fang, "MIMO radar waveform design with PAPR and similarity constraints," *IEEE Trans. Signal Process.*, vol. 66, no. 4, pp. 968–981, Feb. 2018.
- [56] L. Zheng, M. Lops, X. Wang, and E. Grossi, "Joint design of overlaid communication systems and pulsed radars," *IEEE Trans. Signal Process.*, vol. 66, no. 1, pp. 139–154, Jan. 2018.
- [57] P. Stoica, J. Li, and Y. Xie, "On probing signal design for MIMO radar," *IEEE Trans. Signal Process.*, vol. 55, no. 8, pp. 4151–4161, Aug. 2007.
- [58] L. Xu, J. Li, and P. Stoica, "Target detection and parameter estimation for MIMO radar systems," *IEEE Trans. Aerosp. Electron. Syst.*, vol. 44, no. 3, pp. 927–939, Jul. 2008.
- [59] L. Xu, J. Li, and P. Stoica, "Radar imaging via adaptive MIMO techniques," in *Proc. 14th Eur. Signal Process. Conf. (EUSIPCO)*, Florence, Italy, Sep. 2006, pp. 1–5.
- [60] S. Boyd and L. Vandenberghe, *Convex Optimization*. Cambridge, U.K.: Cambridge Univ. Press, 2004.
- [61] Q. Shi, M. Hong, X. Gao, E. Song, Y. Cai, and W. Xu, "Joint source-relay design for full-duplex MIMO AF relay systems," *IEEE Trans. Signal Process.*, vol. 64, no. 23, pp. 6118–6131, Dec. 2016.
- [62] X.-D. Zhang, *Matrix Analysis and Applications*. Cambridge, U.K.: Cambridge Univ. Press, 2017.
- [63] N. D. Sidiropoulos, T. N. Davidson, and Z.-Q. Luo, "Transmit beamforming for physical-layer multicasting," *IEEE Trans. Signal Process.*, vol. 54, no. 6, pp. 2239–2251, Jun. 2006.



Meng Hua received the M.S. degree in electrical and information engineering from the Nanjing University of Science and Technology, Nanjing, China, in 2016, and the Ph.D. degree from the School of Information Science and Engineering, Southeast University, Nanjing, in 2021. He is currently a Post-Doctoral Researcher with the State Key Laboratory of Internet of Things for Smart City, University of Macau. His current research interests include intelligent reflecting surface, integrated sensing and communication, UAV assisted communication, backscatter communication, energy-efficient wireless communication, X-connectivity, cognitive radio networks, secure transmission, and optimization theory. He was a recipient of the Outstanding Ph.D. Thesis Award of the Chinese Institute of Electronics in 2021.



Qingqing Wu (Senior Member, IEEE) received the B.Eng. degree in electronic engineering from the South China University of Technology in 2012, and the Ph.D. degree in electronic engineering from Shanghai Jiao Tong University (SJTU) in 2016.

From 2016 to 2020, he was a Research Fellow at the Department of Electrical and Computer Engineering, National University of Singapore. He is currently an Assistant Professor with the State Key Laboratory of Internet of Things for Smart City, University of Macau. He has coauthored more than 100 IEEE journal articles with 25 ESI highly cited articles and eight ESI hot articles, which have received more than 12,000 Google citations. His current research interests include intelligent reflecting surface (IRS), unmanned aerial vehicle (UAV) communications, and MIMO transceiver design. He was a recipient of the IEEE Communications Society Young Author Best Paper Award in 2021; the Outstanding Ph.D. Thesis Award of the China Institute of Communications in 2017; the Outstanding Ph.D. Thesis Funding in SJTU in 2016; the IEEE ICC Best Paper Award in 2021; and the IEEE WCSP Best Paper Award in 2015. He is the Workshop Co-Chair of IEEE ICC 2019–2022 Workshop on Integrating UAVs into 5G and Beyond,” and the Workshop Co-Chair of IEEE GLOBECOM 2020 and ICC 2021 Workshop on “Reconfigurable Intelligent Surfaces for Wireless Communication for Beyond 5G.” He serves as the Workshops and Symposia Officer for Reconfigurable Intelligent Surfaces Emerging Technology Initiative and Research Blog Officer of Aerial Communications Emerging Technology Initiative. He is the IEEE Communications Society Young Professional Chair in Asia Pacific Region. He was the Exemplary Editor of IEEE COMMUNICATIONS LETTERS in 2019 and an exemplary reviewer of several IEEE journals. He serves as an Associate Editor for IEEE TRANSACTIONS ON COMMUNICATIONS, IEEE COMMUNICATIONS LETTERS, IEEE WIRELESS COMMUNICATIONS LETTERS, IEEE OPEN JOURNAL OF COMMUNICATIONS SOCIETY, and IEEE OPEN JOURNAL OF VEHICULAR TECHNOLOGY. He is the Lead Guest Editor of the IEEE JOURNAL ON SELECTED AREAS IN COMMUNICATIONS ON UAV Communications in 5G and Beyond Networks, and the Guest Editor of the IEEE OPEN JOURNAL OF VEHICULAR TECHNOLOGY on 6G Intelligent Communications, and IEEE OPEN JOURNAL OF COMMUNICATIONS SOCIETY on Reconfigurable Intelligent Surface-Based Communications for 6G Wireless Networks. He was listed as a Clarivate ESI Highly Cited Researcher in 2021, the Most Influential Scholar Award in AI-2000 by Aminer in 2021, and the World’s Top 2% Scientist by Stanford University in 2020 and 2021.



Chong He (Member, IEEE) received the B.Sc. degree in electronic and information engineering and the M.S. degree in electromagnetic and microwave technology from the Huazhong University of Science and Technology, Wuhan, China, in 2007 and 2009, respectively, and the Ph.D. degree in electromagnetic and microwave technology from Shanghai Jiao Tong University, Shanghai, China, in 2015.

From 2016 to 2018, he was a Post-Doctoral Researcher at the Department of Electronic Engineering, Shanghai Jiao Tong University. Since 2019, he has been an Assistant Professor with the School of Electronic Information and Electrical Engineering, Shanghai Jiao Tong University. He has authored or coauthored over 80 papers in IEEE journals and conferences. His research interests include phased arrays, reconfigurable intelligent surface, DOA estimation, wireless location, and multiple access wireless communications. He is a TPC Member of IEEE GC 2020 MWN Symposium and 2021 IEEE Wireless Communications and Networking Conference. He has served as a Reviewer for IEEE TRANSACTIONS ON ANTENNAS AND PROPAGATION, IEEE ANTENNAS AND WIRELESS PROPAGATION LETTERS, IEEE TRANSACTIONS ON VEHICULAR TECHNOLOGY, and IEEE WIRELESS COMMUNICATIONS LETTERS, and a Guest Editor of a Special Issue of the IEEE JOURNAL ON SELECTED AREAS IN COMMUNICATIONS in 2021.



Shaodan Ma (Senior Member, IEEE) received the dual bachelor’s degrees in science and economics and the M.Eng. degree in electronic engineering from Nankai University, Tianjin, China, in 1999 and 2002, respectively, and the Ph.D. degree in electrical and electronic engineering from The University of Hong Kong, Hong Kong, in 2006. From 2006 to 2011, she was a Post-Doctoral Fellow at The University of Hong Kong. Since August 2011, she has been with the University of Macau, where she is currently a Professor. Her research interests

include array signal processing, transceiver design, localization, mmwave communications, and massive MIMO. She was a Symposium Co-Chair of various conferences, including IEEE ICC 2021, 2016, and 2019, IEEE/CIC ICC 2019, and IEEE GLOBECOM 2016. She serves as an Editor for the IEEE TRANSACTIONS ON WIRELESS COMMUNICATIONS, IEEE TRANSACTIONS ON COMMUNICATIONS, IEEE WIRELESS COMMUNICATIONS LETTERS, and *Journal of Communications and Information Networks*.



Wen Chen (Senior Member, IEEE) is currently a Tenured Professor with the Department of Electronic Engineering, Shanghai Jiao Tong University, China, where he is also the Director of the Broadband Access Network Laboratory. He has published more than 120 articles in IEEE journals and more than 120 papers in IEEE conferences, with citations more than 8000 in Google Scholar. His research interests include multiple access, wireless AI, and meta-surface communications. He is a fellow of the Chinese Institute of Electronics. He is the Shanghai

Chapter Chair of IEEE Vehicular Technology Society. He is an Editor of IEEE TRANSACTIONS ON WIRELESS COMMUNICATIONS, IEEE TRANSACTIONS ON COMMUNICATIONS, IEEE ACCESS, and IEEE OPEN JOURNAL OF VEHICULAR TECHNOLOGY. He is the Distinguished Lecturer of the IEEE Communications Society and the IEEE Vehicular Technology Society.